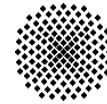
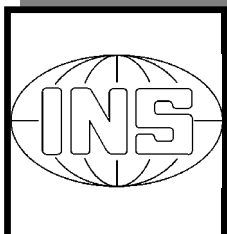


Universität Stuttgart



Schriftenreihe der Institute des Studiengangs Geodäsie und Geoinformatik

Technical Reports
Department of Geodesy and
Geoinformatics



G. Fotopoulos, C. Kotsakis,
M.G. Sideris

Evaluation of Geoid Models
and Their Use in Combined
GPS/Levelling/Geoid Height
Network Adjustments

**Evaluation of Geoid Models and Their Use in
Combined GPS/Levelling/Geoid Height Network
Adjustments**

Prepared by:

G. Fotopoulos, C. Kotsakis, and M.G. Sideris

Department of Geomatics Engineering

The University of Calgary

2500 University Drive N.W.

Calgary, Alberta, Canada T2N 1N4

June 1999

Table of Contents

| | |
|-----------------------------------------------------------------------------------------------------------|----|
| Abstract | 1 |
| 1. Introduction | 2 |
| 2. Development of a New Canadian Geoid Model | 4 |
| 2.1 Computational Methodology | 5 |
| 2.2 GARR98 | 9 |
| 3. Evaluation of Various Geoid Models | 10 |
| 3.1 Comparisons Between Geoid Models | 10 |
| 3.2 Comparisons at GPS Benchmarks | 14 |
| 3.3 Absolute Agreement of Geoid Models with Respect to GPS/Levelling | 15 |
| 3.4 Relative Agreement of Geoid Models with Respect to GPS/Levelling | 19 |
| 3.5 Results from a Kinematic DGPS Campaign..... | 23 |
| 4. Adjustment of Combined GPS/Levelling/Geoid Networks | 25 |
| 4.1 Overview of Various Adjustment Schemes..... | 26 |
| 4.1.1 Geoid Evaluation | 27 |
| 4.1.2 Corrector Surface for GPS/Levelling | 28 |
| 4.1.3 Gravimetric Geoid Refinement | 29 |
| 4.1.4 Vertical Datum Testing/Refinement | 29 |
| 4.2 General Modelling Considerations | 30 |
| 4.3 A General Adjustment Model..... | 32 |
| 4.4 A Purely Deterministic Approach | 37 |
| 4.5 Some Preliminary Numerical Tests of Methods Used for the Adjustment of Combined GLG Networks | 41 |
| 4.5.1 Western Canada | 41 |
| 4.5.2 Eastern Canada..... | 47 |
| 4.5.3 Surface Plots..... | 50 |
| 4.6 A 'Collocation' Approach..... | 52 |
| 4.7 Statistical Testing in GPS/Levelling/Geoid Networks | 58 |
| 5. Concluding Remarks | 63 |
| 6. Acknowledgements | 65 |
| 7. References | 66 |

Abstract

The purpose of this report is to provide a comprehensive evaluation of geoid models and study their use in combined GPS/levelling/geoid height network adjustments. The information obtained from combining the three height data sets (ellipsoidal, orthometric and geoidal heights) is valuable for many applications and can be more efficient and accurate than traditional techniques. The development of a new gravimetric geoid model (GARR98) for Canada and parts of the U.S., created in the Department of Geomatics Engineering at the University of Calgary is presented herein. In addition, the methodology applied for the computation of the new geoid model, and the specific data types that were used, are discussed. GARR98 uses the most current databases available for Canada, namely new additional surface gravity data, a very high resolution DEM model, and a more accurate global geopotential model (EGM96). Detailed comparisons (both absolute and relative) among the new geoid, global geopotential models (OSU91A and EGM96), the latest GSD95 Canadian geoid model developed by the Geodetic Survey Division of Geomatics Canada, and GPS/levelling-derived geoidal undulations, are also presented and explained. Upon the establishment of the accuracy of these geoid models and the differences between them, a detailed and statistically rigorous treatment of adjustment problems in combined GPS/levelling/geoid networks is provided. Finally, some concluding remarks on the findings of this report are included which may give rise to further studies in this area.

1. Introduction

The simple relationship that exists between the three different height types derived from GPS, levelling, and geoid models has been used for many geodetic applications. The combination of GPS heights with geoid heights to derive orthometric heights can be used to eliminate the strenuous and difficult task of precise spirit levelling, especially in mountainous areas where levelling may not be possible due to the rough terrain and the lack of control points. This relationship between the different height data has been employed as a means of computing an intermediate corrector surface used for the optimal transformation of GPS heights and orthometric heights. Gravimetric geoid evaluation studies have also been routinely based on the combination of such heterogeneous height data.

The combination of various height types is unavoidably plagued with the complexities encountered when dealing with data obtained from different sources such as GPS, spirit levelling and gravimetric geoid models. In order to take advantage of the benefits achieved by using these data sets, a detailed evaluation of their accuracy and optimal means for their combination must be performed. In response to this, an evaluation of a new Canadian geoid and an analysis of combined GPS/levelling/geoid height network adjustments is presented in this report.

The purpose of this report is twofold. First, the development and evaluation of a new gravimetric geoid model (GARR98) for Canada, created in the Department of Geomatics Engineering at the University of Calgary is presented. The methodology applied for the computation of the new geoid, and the data types that were used, are discussed. GARR98 uses the most current databases available for Canada, namely, new additional surface gravity data, a high resolution digital elevation model (DEM), and a more accurate global geopotential model (GM), EGM96. Comparisons among the new geoid, pure GM-derived geoids (OSU91A and EGM96), the latest GSD95 Canadian geoid model, and GPS/levelling data, are also presented. Absolute and relative differences at 1307 GPS benchmarks are computed, on both national and regional scales. These external

comparisons reveal interesting information regarding the behavior of the Canadian gravity field, the quality of the geoid models, and the achievable accuracy in view of future GPS/levelling applications.

The second purpose deals with the adjustment of combined GPS/levelling/geoid (GLG) height networks. A detailed and statistically rigorous treatment of adjustment problems in combined GPS/levelling/geoid networks is given in this report. The two main types of ‘unknowns’ in this kind of multi-data 1D networks are usually the gravimetric geoid accuracy and a 2D spatial field that describes all the datum/systematic distortions among the available height data sets. Accurate knowledge of the latter becomes especially important when we consider employing GPS techniques for levelling purposes with respect to a local vertical datum. Two modelling alternatives for the correction field are presented, namely a purely deterministic parametric model, and a hybrid deterministic and stochastic model. The concept of variance component estimation is also proposed as an important statistical tool for assessing the actual gravimetric geoid noise level and/or testing a-priori determined geoid error models.

A brief outline of the methodology used for a new gravimetric geoid model created in the Department of Geomatics Engineering at the University of Calgary will be presented, followed by an evaluation of the absolute and relative accuracies of the geoid model on both national and regional scales. Results of a kinematic GPS campaign performed in a small area just east of the Rocky Mountain region is also included to provide an example of the type of results that are achievable using the new geoid model. The remaining sections of this report concentrate on issues related to adjustment problems in combined GLG networks. Preliminary results from a simple analysis performed using two of the adjustment methods will also be presented which reveal the interesting nature of combined GLG height adjustment problems. Finally, some conclusions about the material presented in this report will be provided which lead to recommendations on future work on this topic.

2. Development of a New Canadian Geoid Model

The benefits achieved from combining GPS measurements with geoid information was the main motivation behind the pursuit of computing a new gravimetric geoid model for Canada and parts of the U.S. Since the last Canadian geoid model, GSD95, was created by the Geodetic Survey Division in 1995 (Veronneau, 1996), new gravity field data has been obtained which can be used to update the geoid information, resulting in a more accurate representation of the Canadian region. The geoid heights (N) obtained from this model could then be used in conjunction with GPS ellipsoidal heights (h), in order to compute orthometric heights (H) practically everywhere in Canada, as shown in the simple equation below and depicted in Figure (2.1):

$$H = h - N \quad (2.1)$$

In the past, traditional spirit levelling has been used to obtain height information with very high accuracy. By nature, spirit levelling is a very time consuming, weather dependent, costly and laborious task. In addition to these shortcomings, spirit levelling is not feasible for obtaining absolute heights in large unsurveyed territories, such as northern Canada, due to the absence of any vertical control. The versatility and accuracy of GPS has brought to the forefront of the surveying industry the importance of an accurate geoid that will allow for the use of GPS/levelling techniques as an efficient alternative over traditional levelling. The following section of this report outlines the data and methodology used for the development of a new Canadian geoid.

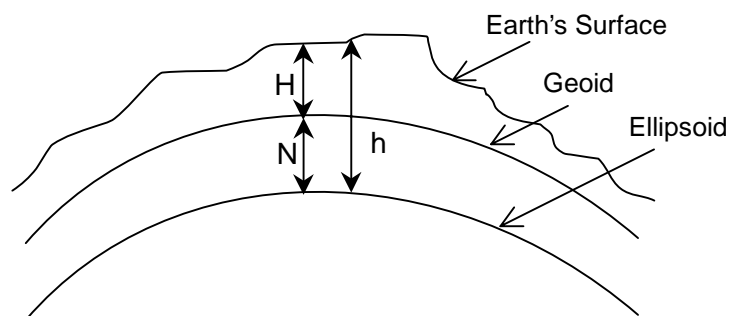


Figure 2.1: Relationship Between Orthometric, Geoid and Ellipsoidal Heights

2.1 Computational Methodology

The computation of the new Canadian geoid model (GARR98) was based on the classical "remove-compute-restore" technique. The underlying procedure can be summarized as follows:

- 1) *Remove* a gravity anomaly field (computed from a global spherical harmonic model evaluated at the geoid) from Helmert gravity anomalies that are computed from local surface gravity measurements and digital elevation data. In this way, "residual Helmert anomalies" are obtained. Faye anomalies were actually used to approximate the Helmert gravity anomalies.
- 2) *Compute* "residual co-geoid undulations" (N_{Ag}) by a spherical Fourier representation of Stokes' convolution integral using the residual gravity anomalies.
- 3) *Restore* a geoid undulation field N_{GM} (computed from a global spherical harmonic model evaluated at the geoid) to the residual co-geoid undulations, and add also a topographic indirect effect term N_H (computed from digital elevation data) to form the final geoid undulations.

The above three steps can be combined in a single formula as follows:

$$N = N_{GM} + N_{Ag} + N_H \quad (2.2)$$

The computation of the N_{GM} term was made on a $5' \times 5'$ grid, within the following geographical boundaries: northern $N72^\circ$, southern $N41^\circ$, western $W142^\circ$, and eastern $W53^\circ$. This is also the grid configuration in which the final GARR98 geoid heights are given. The EGM96 geopotential model (complete to degree and order 360) was used for these computations, according to the following formula (Heiskanen and Moritz, 1967):

$$N_{GM} = R \sum_{n=2}^{360} \sum_{m=0}^n [\bar{C}_{nm} \cos(m\lambda) + \bar{S}_{nm} \sin(m\lambda)] \bar{P}_{nm}(\sin \phi) \quad (2.3)$$

An initial comparison at the above grid between EGM96 and the OSU91A geopotential model which was used in the development of the latest GSD95 Canadian geoid, showed an RMS undulation difference of 97 cm. Further information and tests for the performance of the EGM96 geopotential model over the Canadian region can be found in IGeS (1997). Additional comparisons are presented in the following section of this report.

The medium and small wavelength contributions to the total geoid heights were computed from the local gravity anomaly data, according to Stokes' formula (Heiskanen and Moritz, 1967)

$$N_{\Delta g}(\phi_P, \lambda_P) = \frac{R}{4\pi\gamma} \int_{\lambda_Q \phi_Q} \int \Delta g(\phi_Q, \lambda_Q) S(\psi_{PQ}) \cos \phi_Q d\phi_Q d\lambda_Q \quad (2.4)$$

where $S(\psi)$ is the Stokes function, and the local data Δg are residual Faye anomalies, i.e.

$$\Delta g = \Delta g_{FA} + c - \Delta g_{GM} \quad (2.5)$$

In the last equation, Δg_{FA} are the usual free-air anomalies, c is the terrain correction term, and Δg_{GM} is the removed long wavelength contribution of the geopotential model computed from the expression

$$\Delta g_{GM} = G \sum_{n=2}^{n_{\max}} (n-1) \sum_{m=0}^n (\bar{C}_{nm} \cos m\lambda + \bar{S}_{nm} \sin m\lambda) \bar{P}_{nm}(\sin \varphi) \quad (2.6)$$

where \bar{C}_{nm} and \bar{S}_{nm} are normalized coefficients from a spherical harmonic series expansion for the anomalous potential obtained from a global geopotential model data set (EGM96 or OSU91A) and \bar{P}_{nm} are normalized Legendre functions. All the gravity data were obtained from the Geodetic Survey Division (GSD) of Geomatics Canada in the form of a $5' \times 5'$ grid of mean Faye anomalies, within the same geographical boundaries mentioned above. This is essentially a smaller part of the gravity grid used in the

development of the original GSD95 geoid model. The GSD95 gravity grid covered a slightly larger region, which extended its eastern boundary to W46° and including half of the Greenland area and most of the Labrador Sea. However, the GARR98 grid incorporates some newly obtained surface gravity information across British Columbia, which was not used in the GSD95 solution. The average spacing of the surface gravity measurements used for the gridding was approximately 10 km on land, and 1 km over the oceans in Canada. A detailed description of the Canadian gravity database and the followed gridding procedures can be found in Veronneau (1995 and 1996). A discussion for the treatment and computation of all the necessary gravity reductions (atmospheric, free-air gradient, terrain reduction) applied to the original data is included in Veronneau (1994) and Mainville et al. (1994).

The evaluation of Stokes' integral (2.4) was performed by the 1D spherical FFT algorithm (Haagmans et al., 1993), according to the expression

$$N_{\Delta g}(\phi_p, \lambda_p) = \frac{R\Delta\phi\Delta\lambda}{4\pi\gamma} \mathbf{F}^{-1} \left\{ \sum_{\phi_Q=\phi_1}^{\phi_{max}} \mathbf{F}[S(\psi_{PQ})] \mathbf{F}[\Delta g(\phi_Q, \lambda_Q) \cos\phi_Q] \right\} \quad (2.7)$$

where the operators \mathbf{F} and \mathbf{F}^{-1} denote the forward and inverse 1D discrete Fourier transform, $\Delta\phi = \Delta\lambda = 5'$ is the used grid spacing, and ϕ_1 , ϕ_{max} are the southern and northern grid boundaries, respectively. The gravity anomaly input grid ($\Delta g \cos\phi$) had 50% zero padding applied on the east and west edges of the grid, but none on the north and south sides. This is because equation (2.7) performs the FFT in the east/west direction, and thus padding is only needed on those two edges to eliminate circular convolution effects. On the other hand, the values of the Stokes spherical kernel S were analytically computed at all points of the zero-padded grid, and its discrete spectrum values were subsequently used in (2.7). Also, no tapering of Δg was performed, since the long wavelength part of the gravity anomaly signal had already been removed from the grid values.

The shorter wavelength information for the GARR98 geoid model was obtained through the computation of the indirect effect term N_H , induced by using Helmert's second condensation method for the gravity data reduction on the geoid (Heiskanen and Moritz, 1967). In general, the formulation of the topographic indirect effect on the geoid, according to Helmert's second condensation method, is made in terms of a Taylor series expansion from which only the first three terms are usually considered:

$$N_H = \delta N_o + \delta N_1 + \delta N_2 \quad (2.8)$$

Wichiencharoen (1982) and Sideris (1990) should be consulted for all the detailed formulas. In our case, only the zero-order term

$$\delta N_o = -\frac{\pi G \rho H_{DEM}^2}{\gamma} \quad (2.9)$$

was used for the geoid computations, since it is the dominant one. The same approximation was also adopted in the construction of the GSD95 geoid model. The height data used to evaluate (2.9) were obtained from a $1\text{km} \times 1\text{km}$ Digital Elevation Model (DEM) which covered most of the Western Canadian region ($N67^\circ$, $N47^\circ$, $W135^\circ$, $W110^\circ$). In contrast to the GSD95 geoid solution, which additionally used the global ETOPO5-DEM and the Digital Terrain Elevation Data set (DTED-Level 1) to obtain a total terrain coverage for Canada, no other height data sources were incorporated in the GARR98 model. However, the DEM file that was used in the GARR98 geoid solution provided us with a better overall terrain resolution for the Western mountainous parts of Canada, since it was not restricted only in the Northern British Columbia and in the Yukon Territory, as it happened with the corresponding $1\text{km} \times 1\text{km}$ DEM used in the GSD95 geoid solution (Veronneau, 1996).

2.2 GARR98

The final GARR98 geoid model on a $5' \times 5'$ grid is illustrated in Figure (2.2). Table (2.1) summarizes the statistics of the GARR98 and the GSD95 geoid models. Note that the statistics for the GSD95 model refer to its original grid boundaries (N72°, N41°, W142°, W46°), which differ slightly from the ones used in GARR98.

Table 2.1: Statistics of GSD95 and GARR98 Geoid models

| Geoid model | Minimum | Maximum | Mean | σ | RMS |
|----------------------|---------|---------|--------|----------|-------|
| All values in metres | | | | | |
| <i>GARR98</i> | -47.66 | 48.46 | -14.55 | 20.30 | 24.97 |
| <i>GSD95</i> | -49.00 | 43.88 | -15.45 | 20.04 | 25.30 |

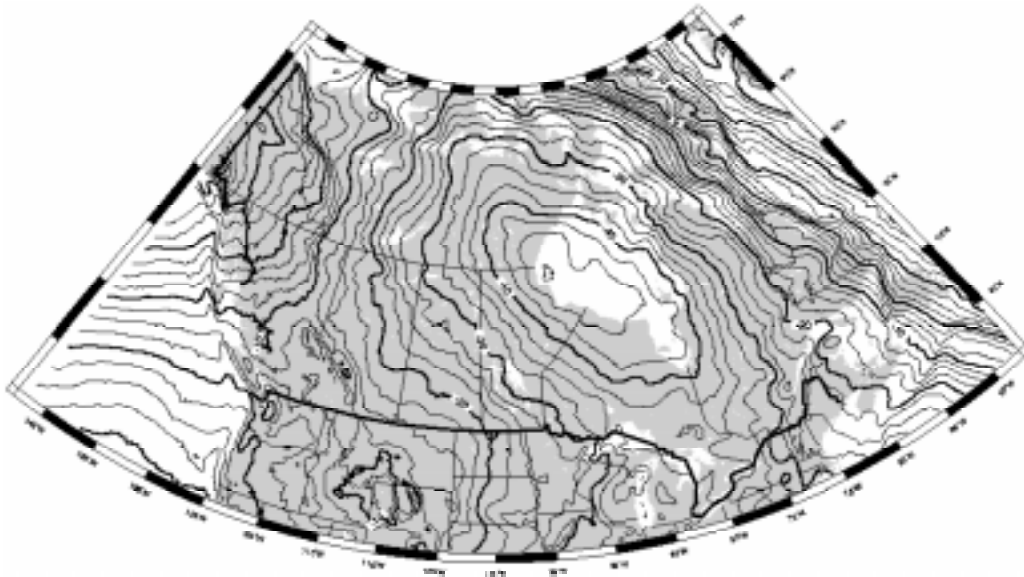


Figure 2.2: The GARR98 Geoid Model (contour interval: 2.5 m)

3. Evaluation of Various Geoid Models

An important aspect during the development of a new gravimetric geoid for Canada was its evaluation with already existing geoid models. Comparisons between GARR98 and other models (GSD95, EGM96 and OSU91A) were conducted in order to assess the accuracy of the models on both regional and national scales. In addition to inter-comparisons between models, results for the absolute and relative agreement of these geoid models with respect to GPS/levelling data are also provided. Finally, a sample of the achievable orthometric height accuracies resulting by combining GPS heights derived from a kinematic DGPS campaign and geoid heights, is provided to demonstrate the feasibility of performing actual ‘GPS/levelling’.

3.1 Comparisons Between Geoid Models

In order to investigate the quality of the new gravimetric geoid, comparisons between various geoid models were made by differencing their geoidal undulation values on the 5' \times 5' grid used to compute GARR98 (see Section 2.2). These differences are displayed graphically on shaded contour plots in Figures (3.1) through (3.3), and their statistics are given in Table (3.1).

At first, a comparison between the EGM96 and OSU91A global geoid models is made, and the result is illustrated in Figure (3.1). It reveals the strong effect of the additional gravity data in the Western and in the Northeastern parts of Canada, which were incorporated in the development of EGM96. This new gravity data results in up to 10 metre differences in geoidal undulations in Northwestern Canada and the area around Greenland. Extreme differences are also seen in the Rocky Mountain region due to its rugged terrain features, which suggests the importance of using dense gravity coverage in order to recover the small-wavelength gravity field information. The highest level of agreement between the two global models is found in Central Canada averaging up to 50 cm, which increases to up to 1.5 m in parts of Eastern Canada.

Figure (3.2) shows the differences between GSD95 and EGM96, which basically reveal the medium and small wavelength structure of the Canadian gravity field, combined with the discrepancies between EGM96 and OSU91A. It should be kept in mind that GSD95 uses the OSU91A model as a reference field. Again, the maximum differences between the models are seen in the Western mountainous regions, as well as in the Northeastern areas.

The differences between the two gravimetric solutions, GARR98 and GSD95, are shown in Figure (3.3). The RMS agreement of those two geoid models is at the 37 cm level. The largest difference values averaging 1-2 m, with a maximum of up to 4 m, are seen in the Hudson Bay area as well as the shores of the Grand Banks area around the Davis Strait which is located on the Northeastern coast of Canada. These differences can be partly correlated to the differences between the two global models (see Figure 3.1), as well as to the extended gravity grid used for GSD95 up to W46° as opposed to W53° for GARR98. The geoids have the highest level of agreement in the Canadian Shield area, Central BC, Southern Alberta, Saskatchewan and Northern Quebec.

Table 3.1: Statistics for Various Geoid Models and Their Differences

| Geoid model | Minimum | Maximum | Mean | σ | RMS |
|--------------------------------|----------------|----------------|-------------|----------------------------|------------|
| All values in metres | | | | | |
| <i>GARR98</i> | -47.66 | 48.46 | -14.55 | 20.30 | 24.97 |
| <i>GSD95</i> | -49.00 | 43.88 | -15.45 | 20.04 | 25.30 |
| <i>EGM96</i> | -48.91 | 48.50 | -15.44 | 20.04 | 25.30 |
| <i>OSU91A</i> | -48.71 | 44.59 | -15.44 | 20.14 | 25.37 |
| Geoid Model Differences | | | | | |
| <i>EGM96-OSU91A</i> | -10.57 | 6.95 | -0.07 | 0.96 | 0.97 |
| <i>GSD95-EGM96</i> | -5.45 | 5.99 | -0.01 | 0.58 | 0.58 |
| <i>GARR98-GSD95</i> | -1.62 | 3.62 | 0.00 | 0.37 | 0.37 |

The areas with the highest levels of disagreement are located in the Northwest Territories, the northern tip of Labrador. The coastal range surrounding the Vancouver area is also fairly poor in terms of agreement. The range of differences in the Western region is approximately 25-50 cm in parts of BC and reduces to 0-25 cm moving north. This may partly be attributed to the higher resolution DEM for these areas, used for the creation of

GARR98 as opposed to the GSD95 geoid, as well as to the newer gravity information obtained for GARR98. The effect of the large discrepancies, noted between the two global models (see Figure 3.1), are also seen on a smaller scale in this western region.

In general, from Figures (3.1) through (3.3), the largest discrepancies between the models occur in the western and northern parts of Canada. The differences in western Canada may be due to the Rocky Mountain range, where undulations change quickly due to terrain effects as noted by the rapid changes visible in the plots. In northern Canada, very sparse gravity measurements have been gathered, hence the computed gravity anomalies are poor affecting both the geopotential coefficients and the local geoid models.

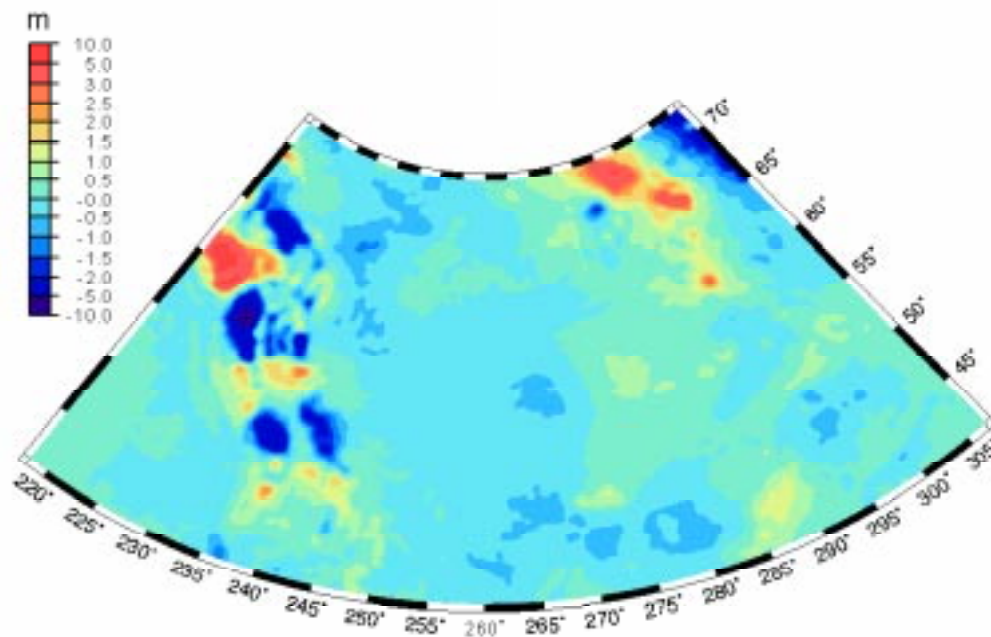


Figure 3.1: Geoid Differences Between EGM96 and OSU91A

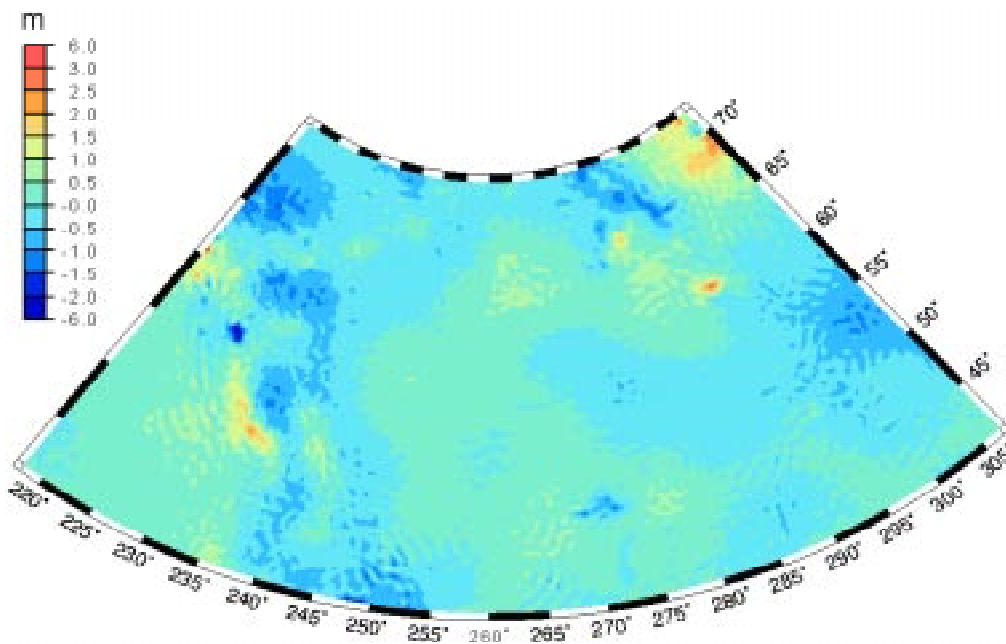


Figure 3.2: Geoid Differences Between GSD95 and EGM96

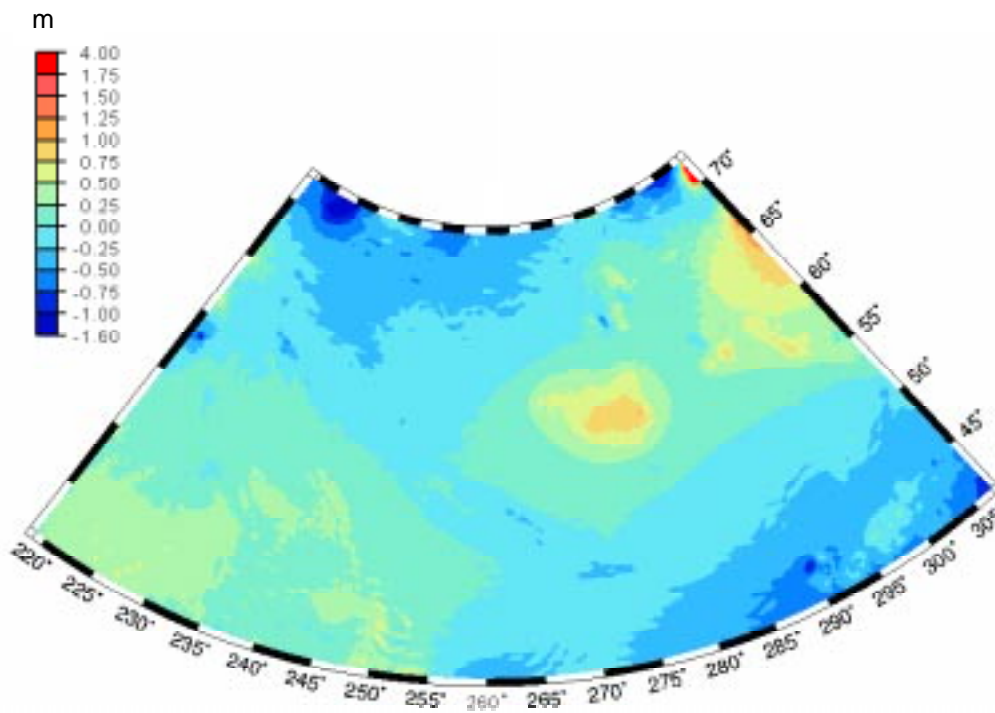


Figure 3.3: Geoid Differences Between GARR98 and GSD95

3.2 Comparisons at GPS Benchmarks

An external evaluation for the quality of a gravimetric geoid model can be performed by comparing its interpolated values (N) at a network of GPS benchmarks with the corresponding GPS/levelling-derived geoid heights (N^{GPS}). Such a comparison is traditionally based on the following model (see, e.g., Forsberg and Madsen, 1990; Sideris et al., 1992):

$$N_i^{GPS} - N_i = h_i - H_i - N_i = x_0 + x_1 \cos \varphi_i \cos \lambda_i + x_2 \cos \varphi_i \sin \lambda_i + x_3 \sin \varphi_i + v_i \quad (3.1)$$

which is solved for the unknown parameters (x_0, x_1, x_2, x_3) by minimizing the quantity $\mathbf{v}^T \mathbf{v}$. The adjusted values for the residuals v_i give a realistic picture of the level of absolute agreement between the gravimetric geoid and the GPS/levelling data. The four-parameter model in (3.1) absorbs most of the datum inconsistencies among the available height data sets, as well as possible long wavelength geoid errors. In such comparisons, it should always be kept in mind that the final residual values v_i are not purely gravimetric geoid determination error, but contain levelling and GPS positioning errors as well. A detailed description of the above transformation model, along with its geometrical interpretation, can be found in Heiskanen and Moritz (1967, p. 213). Further investigations of how this transformation applies to combined GPS/levelling/geoid networks is provided in Section 4 of this report.

A total of 1300 GPS benchmark points (with the outliers removed), which are all part of the first-order Canadian levelling network, were used for the evaluation. Figure (3.4) shows the distribution of these GPS benchmarks across Canada, which varies from a very dense network in the Western regions and along the Trans-Canada highway, to very few points in the Ontario province and in the Northern areas.



Figure 3.4: Distribution of GPS Benchmarks in Canada

The known ellipsoidal height values (h_i) refer to the ITRF92 reference frame. The H_i values correspond to Helmert orthometric heights, computed from true surface gravity measurements and by a minimal-constraint adjustment of the whole Canadian levelling network, where a single point in Rimouski, Quebec, was held fixed. The adjustment was performed by GSD in October 1995, in an attempt to improve the Canadian Vertical Geodetic Datum of 1928 (CVGD28), in view of various systematic distortions accumulated over the years (e.g., mean sea level rise, post glacial rebound, use of approximate normal gravity values instead of true surface gravity measurements in the CVGD28 datum, etc.). Four geoid models were used for the comparisons at the GPS benchmarks, namely, GARR98, GSD95, EGM96, and OSU91A. Both absolute and relative differences were computed with respect to the GPS/levelling-derived geoid, and all the results are presented in the next two sections.

3.3 Absolute Agreement of Geoid Models With Respect to GPS/Levelling

The statistics of the absolute differences between the four geoid models and the GPS/levelling-derived geoid for the entire Canadian region are shown in Table (3.2).

Three additional tables are given, in which the absolute agreement is studied for three separate major regions in Canada. Table (3.3) refers to all GPS benchmarks in Alberta and British Columbia (Western Canada); Table (3.4) uses all the GPS benchmarks lying inside the meridian zone $95^{\circ}\text{W} < \lambda < 110^{\circ}\text{W}$ (Central Canada); and finally Table (3.5) takes into account only the GPS benchmarks east of 95°W (Eastern Canada). Note that the values inside the parentheses, shown in all four tables, are the results after the least-squares fitting of the 4-parameter transformation model has been applied to the original differences. It should be noted that for the computation of all statistics presented in this section, the GPS benchmarks showing large differences before the least-squares fitting (i.e., $>3\sigma$ level) were removed. The removal of such points with gross errors, in either the GPS or levelling data, further improved the results obtained in previous computations where no effort to remove the outliers was performed.

From the statistics shown in Table (3.2), it can be seen that the GARR98 gravimetrically derived geoid, with the support of the EGM96 global model, drastically improves the overall agreement with the GPS/levelling-derived geoid in Canada, from a σ of 44 cm to a σ of 20 cm. After the fit, however, both GARR98 and GSD95 present approximately the same overall external accuracy, which is at the 13-14 cm level. This would suggest that even with the use of EGM96, the present gravity data accuracy and resolution still needs to be improved in Canada, in order to bring the absolute geoid consistency with GPS/levelling data down to the cm-level. It is also interesting to note the superiority of the EGM96 global model, over OSU91A, for describing the long wavelength structure of the Canadian gravity field. After the fit, EGM96 alone fits the Canadian GPS/levelling geoid with an overall RMS accuracy of 31 cm, whereas OSU91A cannot perform better than 67 cm on a national scale (more than 100% difference in accuracy). This is basically due to the fact that OSU91A provides a very poor representation of gravity field features over the British Columbia and Alberta regions, as seen from the corresponding values in Table (3.3).

A regional analysis for the statistics of the differences reveals the interesting result of having the same level of absolute agreement (after fit) for the gravimetric geoid solutions

in both Western and Eastern Canada. This is not surprising and it simply confirms that the strong terrain gravity signal in the Western region has been properly modeled in both GSD95 and GARR98 models. For the same area, the two global geoid models provide an RMS agreement with the GPS/levelling data of 38 cm (EGM96) and 67 cm (OSU91A), respectively, illustrating again the superiority of the EGM96 model.

In Central Canada, GSD95 seems to perform slightly better than GARR98, with the former model giving an after fit RMS accuracy at the GPS benchmarks of 6 cm and the latter 9 cm. A possible reason for this difference in accuracy between the two gravimetric models may be the incorporation in the GSD95 solution of height data for this region, in contrast to GARR98 which uses a DEM only for western Canada. In addition, no improvement in EGM96 over OSU91A occurs in this area, which might have been reflected in the corresponding local gravimetric solutions.

More interesting, however, is the fact that the use of GPS, in conjunction with a global geoid model alone, seems to be sufficient for levelling applications in central Canada requiring dm-level of accuracy. Both global models represent the gravity field in the central flat areas quite well, with an agreement level of 12 cm for both EGM96 and OSU91A. All four geoid models achieve their best performance in this area. For the Eastern part of Canada, both gravimetric geoids show similar results, with GSD95 (12 cm) being marginally better than GARR98 (13 cm). Again, the fact that additional gravity and height data in this region were used in the GSD95 solution (see Section 2) is probably causing this difference. In the case where a global geoid model is only employed for the Eastern region, the level of agreement worsens by more than 10 cm, reaching 24 cm for both EGM96 and OSU91A.

In general, the GARR98 geoid model shows a large bias before the four-parameter transformation (see also table 3.1). For example, in the Eastern region the difference in the mean values between GARR98 and GSD95 is more than 1 m, whereas in the Western region this difference drops to less than 50 cm. These high biased values are not due to the differences between EGM96 and OSU91A, but rather they exist because of the more

extended gravity and height data grids that were used in the computation of GSD95 and not in GARR98 (as described in Section 2.1). The mean value for GARR98 differences decreases as we move west, which is expected since both gravimetric models used the same local gravity and height data in British Columbia and Alberta.

Table 3.2: Comparison of Various Geoid Models with the GPS/levelling Derived Geoid (All of Canada)

| Geoid model | Minimum | Maximum | Mean | σ | RMS |
|----------------------|---------------|--------------|--------------|-------------|-------------|
| All values in metres | | | | | |
| $N^{GPS} - GARR98$ | -2.31 (-0.64) | -1.20 (0.50) | -1.77 (0.00) | 0.20 (0.14) | 1.78 (0.14) |
| $N^{GPS} - GSD95$ | -1.89 (-0.45) | 0.04 (0.54) | -1.13 (0.00) | 0.44 (0.13) | 1.21 (0.13) |
| $N^{GPS} - EGM96$ | -2.55 (-1.27) | 0.41 (1.63) | -1.09 (0.00) | 0.37 (0.31) | 1.15 (0.31) |
| $N^{GPS} - OSU91A$ | -5.92 (-4.73) | 4.04 (5.13) | -1.14 (0.00) | 0.69 (0.67) | 1.34 (0.67) |

Table 3.3: Comparison of Various Geoid Models with the GPS/levelling Derived Geoid (BC and Alberta)

| Geoid model | Min | Max | Mean | σ | RMS |
|----------------------|---------------|--------------|--------------|-------------|-------------|
| All values in metres | | | | | |
| $N^{GPS} - GARR98$ | -2.18 (-0.35) | -1.47 (0.36) | -1.84 (0.00) | 0.11 (0.11) | 1.85 (0.11) |
| $N^{GPS} - GSD95$ | -1.89 (-0.40) | -0.92 (0.39) | -1.39 (0.00) | 0.13 (0.11) | 1.39 (0.11) |
| $N^{GPS} - EGM96$ | -2.55 (-1.24) | 0.41 (1.56) | -1.24 (0.00) | 0.39 (0.38) | 1.30 (0.38) |
| $N^{GPS} - OSU91A$ | -5.92 (-4.67) | 1.49 (2.82) | -1.35 (0.00) | 0.68 (0.67) | 1.52 (0.67) |

Table 3.4: Comparison of Various Geoid Models with the GPS/levelling Derived Geoid (Central Canada)

| Geoid model | Minimum | Maximum | Mean | σ | RMS |
|----------------------|---------------|--------------|--------------|-------------|-------------|
| All values in metres | | | | | |
| $N^{GPS} - GARR98$ | -2.14 (-0.18) | -1.59 (0.31) | -1.91 (0.00) | 0.10 (0.09) | 1.92 (0.09) |
| $N^{GPS} - GSD95$ | -1.65 (-0.22) | -1.15 (0.16) | -1.37 (0.00) | 0.08 (0.06) | 1.37 (0.06) |
| $N^{GPS} - EGM96$ | -1.63 (-0.49) | -0.79 (0.28) | -1.05 (0.00) | 0.13 (0.12) | 1.06 (0.12) |
| $N^{GPS} - OSU91A$ | -1.48 (-0.40) | -0.83 (0.31) | -1.12 (0.00) | 0.14 (0.12) | 1.13 (0.12) |

Table 3.5: Comparison of Various Geoid Models with the GPS/levelling Derived Geoid (Eastern Canada)

| Geoid model | Min | Max | Mean | σ | RMS |
|----------------------|---------------|--------------|--------------|-------------|-------------|
| All values in metres | | | | | |
| $N^{GPS} - GARR98$ | -2.31 (-0.49) | -1.20 (0.44) | -1.58 (0.00) | 0.22 (0.13) | 1.60 (0.13) |
| $N^{GPS} - GSD95$ | -1.31 (-0.49) | 0.04 (0.43) | -0.55 (0.00) | 0.30 (0.12) | 0.63 (0.12) |
| $N^{GPS} - EGM96$ | -1.59 (-0.67) | 0.12 (0.89) | -0.83 (0.00) | 0.25 (0.24) | 0.87 (0.24) |
| $N^{GPS} - OSU91A$ | -1.61 (-0.64) | -0.05 (0.83) | -0.86 (0.00) | 0.28 (0.24) | 0.90 (0.24) |

An interesting observation can also be made by comparing the standard deviation values shown in Tables (3.2) through (3.5), before and after the four-parameter model adjustment. By doing such a comparison one sees that in Western and Central Canada the accuracy improvement for all four geoid models, after the 4-parameter transformation, is approximately constant and averages to about 1.75 cm. This amount is also very close to the mean accuracy improvement for the two global models, occurring in Eastern Canada. It is quite reasonable to assume that such a small amount should represent the difference between the GPS datum and the datum used in the development of the global geoid models, i.e., the reference frame realized by the satellite tracking station coordinates. However, in Eastern Canada both GARR98 and GSD95 exhibit a large deviation from this “1.75 cm accuracy improvement” trend, as it is seen from their corresponding values in Table (3.5). This deviation could possibly be attributed to the fact that the parametric model of eq.(3.1) not only eliminates the datum differences among the available data sets, but also absorbs a part of gravimetric geoid *random* error, caused from the extended amount of low-quality shipborne gravity data used in this area (see Section 4 for details).

3.4 Relative Agreement of Geoid Models With Respect to GPS/Levelling

In order to evaluate the relative accuracy of the four geoid models with respect to the GPS/levelling data, relative undulation differences ($\Delta N - \Delta N^{GPS}$) in parts per million (ppm) were formed for all baselines between the GPS benchmarks, and plotted as a function of the baseline length. Figures (3.5) through (3.8) illustrate these relative differences for all of Canada and for the three separate regions considered in the previous section. The relative differences refer to the values obtained after filtering the GPS/levelling benchmarks for outliers and after the fitting of the transformation model (3.1), as described previously.

On a national scale (Figure 3.5), the two global geopotential models show similar relative accuracies up to baseline lengths of 350 km, ranging from 3.5 ppm (20 km) to 0.5 ppm (300-350 km). For larger baseline lengths, we begin to see the improved long wavelength

structure of EGM96 as compared to OSU91A, with EGM96 giving approximately 0.3 ppm for up to 1500 km baselines, and OSU91A averaging to about 0.5 ppm for the same baseline-length band. For larger than 1500 km baselines, both models start dropping to approximately 0.2 ppm.

GARR98 and GSD95 exhibit similar behavior across Canada for all baseline lengths, which is approximately 2.5 ppm for baselines of 20 km, 1.3 ppm for baselines of 100 km, dropping down to 1 ppm at approximately 250 km, and 0.2 ppm for baseline lengths over 500 km. In all cases, some remaining long wavelength errors are evident in Figure 3.5.

In British Columbia and Alberta GARR98 and GSD95 perform essentially the same. For baseline lengths up to 20 km their relative accuracy is at the 2.5 ppm level, decreasing to 0.8 ppm for baseline lengths of 100 km. The relative accuracy for baseline lengths of 200 km drops to approximately 0.4 ppm and at 400 km has reached the 0.2 ppm level, which remains almost constant for up to 800 km baselines. A slightly better performance of GARR98 over GSD95, seen in some parts of Figure 3.6, can be attributed to the improved long wavelength structure of EGM96 over OSU91A for Western Canada. The large difference between the performance of the two global geoid models in this region can also be seen in the long baseline lengths (>300 km), where there is an average of 0.5 ppm improvement in EGM96's relative accuracy over OSU91A. EGM96 also seems to be able to minimize the long wavelength errors that are so pronounced in OSU91A.

As we move eastwards, larger differences between GARR98 and GSD95 become more evident. In Central Canada (Figure 3.7), GSD95 performs better than GARR98 by approximately 0.5 ppm for baseline lengths up to 480 km, and this difference decreases to an average of 0.1 ppm for baseline lengths 500-800 km.

In Eastern Canada, GSD95 seems to perform better the GARR98 for shorter baselines averaging 2.5 ppm at 20 km baselines while GARR98 averages 3.5 ppm for the same baseline length. The difference in relative accuracy between models decreases as the baseline length increases. After 200 km both models seem to perform essentially the

same averaging 0.3 ppm for baseline lengths up to 1500 km. The performance of the two geopotential models is similar for all baselines with the exception of baseline lengths of 100-450 km where EGM96 seems to perform approximately 0.3 ppm better than OSU91A. For baseline lengths greater than 450 km both models have relative accuracies of approximately 0.5 ppm. The differences in relative accuracies between the various models demonstrates the importance of incorporating extended gravity and height information in gravimetric geoid solutions for large areas (like Canada), in order to achieve the level of accuracy required for substituting conventional spirit levelling by GPS techniques.

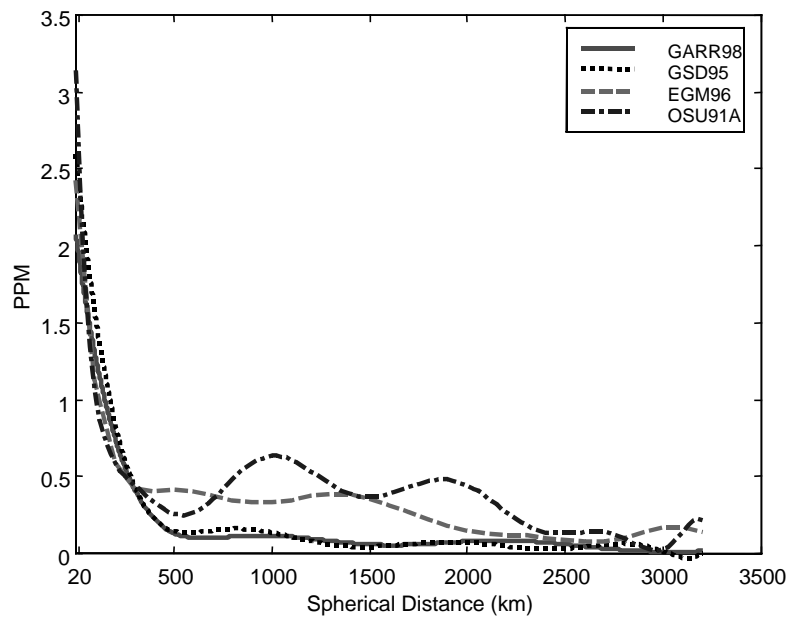


Figure 3.5: Relative Accuracy of the Geoid Models Across Canada

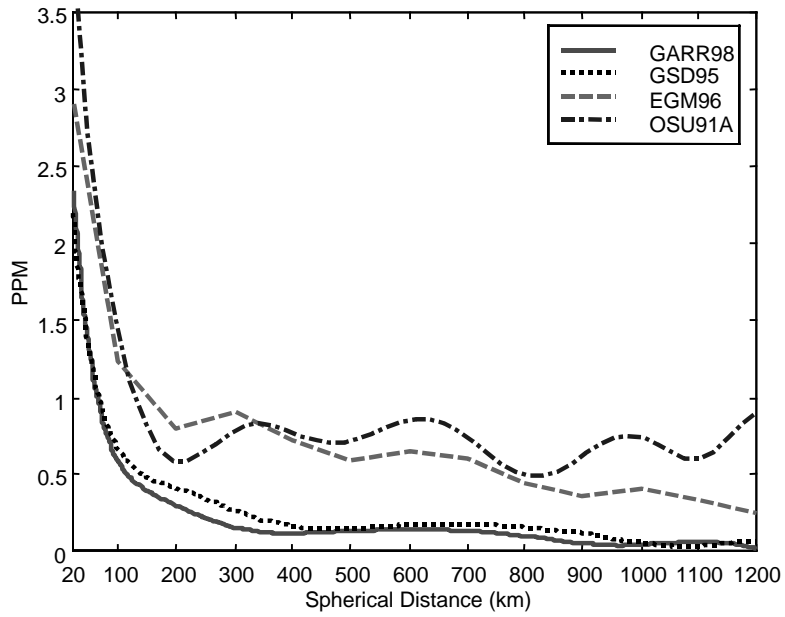


Figure 3.6: Relative Accuracy of the Geoid Models in BC and Alberta

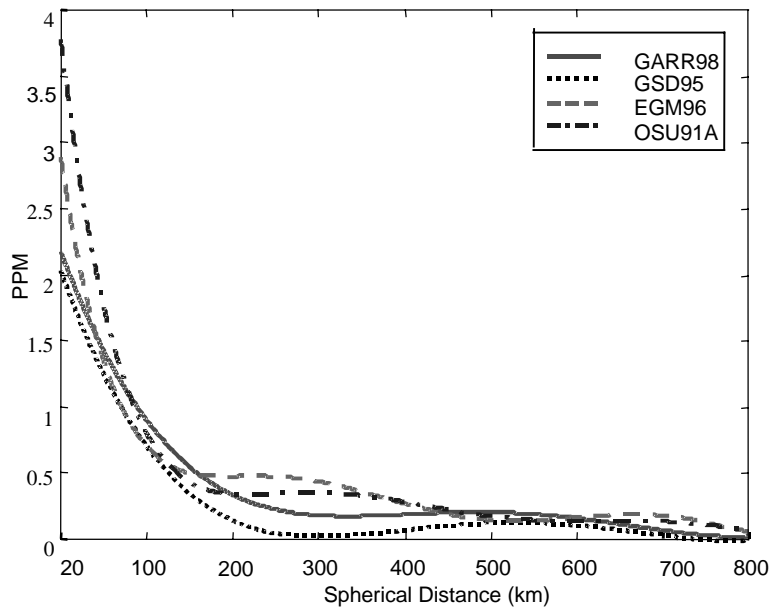


Figure 3.7: Relative Accuracy of the Geoid Models in Central Canada

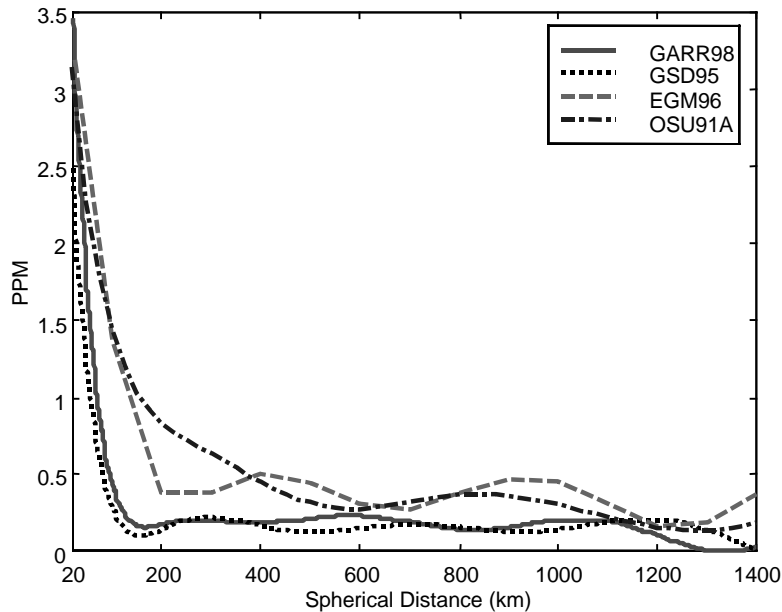


Figure 3.8: Relative Accuracy of the Geoid Models in Eastern Canada

3.5 Results from a Kinematic DGPS Campaign

On January 31, 1998, an eight-hour kinematic DGPS campaign was conducted in order to assess the accuracy of the published orthometric heights as compared to the heights obtained by combining GPS and the new geoid model for a small test network. The network is situated in southwestern Alberta, just east of the Rocky Mountain Range in an area known as the Foothills. The entire network spanned a $15' \times 25'$ area between $51^{\circ}00'00$ to $51^{\circ}15'00$ North latitude and $114^{\circ}20'00$ to $114^{\circ}45'00$ West longitude. The ASCM height difference between the highest and lowest points in the network is approximately 298.5 metres. The region was selected because a number of existing Alberta Survey Control Monuments (ASCM) were readily available with published orthometric heights, which were used for comparing with the results obtained from the GPS campaign.

The results for six remote stations located in this network are presented in Table (3.6). Two NovAtel MiLLennium™ receivers were used for collecting the GPS data at one second intervals. The ellipsoidal heights of the remote stations were obtained in post-

mission by post-processing using a differential carrier-phase fixed solution. A base station was situated on a pillar located on the roof of the Engineering building at the University of Calgary, located approximately 40 km from the network. In all cases, the geoid height refers to the values obtained from GARR98 model, interpolated at the points of interest.

Table 3.6: Orthometric Height Results from Kinematic DGPS Campaign

| Station ID | Latitude (dms) | Longitude (dms) | ASCM Height (m) | Geoid Height (m) | Ellipsoidal Height (m) | ΔH (m) |
|------------|----------------|-----------------|-----------------|------------------|------------------------|----------------|
| 26195 | 51°15'19" | -114°33'34" | 1308.575 | -15.913 | 1292.693 | -0.031 |
| 165472 | 51°11'01" | -114°41'54" | 1301.356 | -15.465 | 1285.869 | 0.022 |
| 338848 | 51°10'59" | -114°33'36" | 1241.371 | -15.974 | 1225.41 | -0.013 |
| 238394 | 51°02'16" | -114°29'18" | 1266.121 | -15.905 | 1250.318 | -0.102 |
| 1917 | 51°01'17" | -114°22'25" | 1183.933 | -16.129 | 1167.75 | 0.054 |
| 419440 | 51°07'40" | -114°33'16" | 1277.161 | -15.912 | 1261.178 | 0.071 |

It should be noted that the ASCM stations were established using various levelling techniques including, inertial surveying systems (ISS), GPS, and spirit levelling methods. In Table (3.6), the first two stations were established using ISS, the next three stations were established using GPS and the last station was established using spirit levelling. These different methods are important since the associated accuracy of the height information varies depending on the method employed for establishing the ASCM height. The approximate accuracy of the points established using ISS is at the metre level, while the points established using GPS are accurate to approximately 2 to 5 cm. The spirit levelled points depend on the order of levelling which typically produces accuracies of 1 to 15 cm. The final column in the table represents the residual values computed between the published ASCM orthometric heights and the height obtained by combining the GPS and geoid information. On average the results agree to within 5 cm. However, a larger network consisting of a greater number of stations must be used in order to achieve more reliable results. Although a reliable account of the absolute accuracies achieved from this kinematic DGPS campaign is not possible from a small set of six stations, further tests may provide more insight as to whether this method is a feasible alternative to traditional levelling.

4. Adjustment of Combined GPS/Levelling/Geoid Networks

The combined use of GPS, levelling, and geoid information has been a key procedure for various geodetic applications. Although these three types of height information are considerably different in terms of physical meaning, reference surface definition/realization, observational methods, accuracy, etc., they should fulfill the simple geometrical relationship (see also equation 2.1):

$$h - H - N = 0 \quad (4.1)$$

where h , H , and N are as described in Section 2.1. In practice equation (4.1) is never satisfied due to (i) *random noise in the values of h , H , N* , (ii) *datum inconsistencies and other possible systematic distortions in the three height data sets* (e.g. long-wavelength systematic errors in N , distortions in the vertical datum due to an overconstrained adjustment of the levelling network, deviation between gravimetric geoid and reference surface of the levelling datum, etc.), (iii) *various geodynamic effects* (post glacial rebound, land subsidence, plate deformation near subduction zones, mean sea level rise, monument instabilities), and (iv) *theoretical approximations in the computation of either H or N* (e.g. improper or omitted terrain/density modeling in the geoid solution, improper evaluation of Helmert's formula for orthometric heights using normal gravity values instead of actual surface gravity observations, negligence of the Sea Surface Topography (SST) at the tide gauges, error-free assumption for the tide gauge observations, etc.). The statistical behavior and modelling of the misclosures of equation (4.1), computed in a network of levelled GPS benchmarks, have been the subject of many studies which are often considerably different in terms of their research objectives. The following is a non-exhaustive list for some of these objectives. The references provided are just representative and not the only important ones.

- (1) Testing the performance of global spherical harmonic models for the Earth's gravitational field (IGeS, 1997), or testing the performance of local/regional

gravimetric geoid models and their associated computational techniques (Mainville et al., 1992; Sideris et al., 1992).

- (2) Development of intermediate corrector surfaces for optimal height transformation between geoid surface and levelling datum surface (Mainville et al., 1997; Smith and Milbert, 1996).
- (3) Development of corrector surfaces for low-wavelength gravimetric geoid errors (De Bruijne et al., 1997), and general gravimetric geoid refinement strategies (Jiang and Duquenne, 1996).
- (4) Evaluation of the achievable accuracy for 'levelling by GPS' surveys (Forsberg and Madsen, 1990).
- (5) Monitoring, testing, and/or improving (strengthening) of already existed vertical datums (Hein, 1986; Kearsley et al., 1993).

The above list can be further extended if we substitute the GPS height h in equation (4.1) with altimetric observations, and the orthometric height H with the SST. A study for such marine applications is included in De Bruijne et al. (1997). In view of the many different uses for such multi-data 1D networks, the purpose of this section is to present some general adjustment and modelling schemes that can be employed for an optimal analysis of the misclosures of equation (4.1). In particular, we are mainly interested in applications of the type (1), (2), or (3) from the previous list.

4.1 Overview of Various Adjustment Schemes

A brief review of various adjustment and modelling schemes, that have been already applied for the applications mentioned in the previous section, will be given here. Some general aspects for adjustment problems with combined height data sets can be found in Pelzer (1986).

4.1.1 Geoid Evaluation

Most of the geoid evaluation studies, based on comparisons with GPS/levelling data, make use of the following basic model:

$$h_i - H_i - N_i = \mathbf{a}_i^T \mathbf{x} + v_i \quad (4.2)$$

where \mathbf{x} is a vector of n unknown parameters, \mathbf{a}_i is an $n \times 1$ vector of known coefficients, and v_i denotes a residual random noise term. The parametric part $\mathbf{a}_i^T \mathbf{x}$ is supposed to describe all possible datum inconsistencies and other systematic effects in the data sets. In practice, for these studies, the usual four-parameter model is often used, i.e.

$$\mathbf{a}_i^T \mathbf{x} = x_0 + x_1 \cos \varphi_i \cos \lambda_i + x_2 \cos \varphi_i \sin \lambda_i + x_3 \sin \varphi_i \quad (4.3)$$

and rarely its five-parameter extension (see, e.g., Duquenne et al., 1995)

$$\mathbf{a}_i^T \mathbf{x} = x_0 + x_1 \cos \varphi_i \cos \lambda_i + x_2 \cos \varphi_i \sin \lambda_i + x_3 \sin \varphi_i + x_4 \sin^2 \varphi_i \quad (4.4)$$

has also been employed. Both equations (4.3) and (4.4) correspond to the following datum transformation model for the geoid undulation N , which is described extensively in Heiskanen and Moritz (1967, sec.5-9):

$$\Delta N_i = \Delta a + \Delta X_0 \cos \varphi_i \cos \lambda_i + \Delta Y_0 \cos \varphi_i \sin \lambda_i + \Delta Z_0 \sin \varphi_i + a \Delta f \sin^2 \varphi_i \quad (4.5)$$

where $\Delta X_0, \Delta Y_0, \Delta Z_0$ are the shift parameters between two ‘parallel’ datums and $\Delta f, \Delta a$ are the changes in flattening and semi-major axis of the corresponding ellipsoids. In our case, the two different datums will correspond to (i) the GPS datum and (ii) the datum used for the development of the global spherical harmonic model that supports the gravimetric geoid, and for the computation of the gravity anomaly data Δg . The model of

equation (4.2) is applied to all network points and a least-squares adjustment is performed to estimate the residuals v_i , which are traditionally taken as the final external indication of the geoid accuracy. The main problem under this approach is that the v_i terms will contain a combined amount of GPS, levelling, and geoid random error, that needs to be separated into its individual components for a more reliable geoid assessment. Furthermore, an optimal adjustment in a statistical sense would require the proper weighting of the residuals, which is hardly applied in practice. Finally, the use of such oversimplified parametric models, like (4.3) or (4.4), combined with improper weighting of the residuals v_i , create important problems in terms of the ‘separability’ of the various random and systematic effects between the two unknown components $\mathbf{a}_i^T \mathbf{x}$ and v_i .

4.1.2 Corrector Surface for GPS/levelling

The development of such corrector surfaces aims basically at providing GPS users with an optimal transformation model between ellipsoidal heights h and orthometric heights H with respect to a given levelling datum. For a general discussion regarding theoretical and practical aspects of this problem, see Featherstone (1998). Two such developments have been reported in North America, particularly in the U.S. by the National Geodetic Survey (NGS; Smith and Milbert, 1996) and in Canada by the Geodetic Survey Division (GSD; Mainville et al., 1997). Both studies followed a similar methodology, using initially the basic model of equation (4.2) with its parametric part given by equation (4.3). The obtained adjusted values for the residuals v_i were then spatially modelled in a grid form using an interpolation procedure. In the GSD study, a minimum-curvature interpolation algorithm was used, whereas NGS fitted an isotropic Gaussian covariance function to the statistics of the irregularly distributed values v_i and then used simple collocation formulas for the gridding. From the combination of the gridded values for the residuals and the adjusted values for the parameters \mathbf{x} , a corrector surface was finally computed. Some comments regarding the drawbacks of these modelling approaches will be given later on in this chapter.

4.1.3 Gravimetric Geoid Refinement

In De Bruijne et al. (1997), a 28-parameter surface model was estimated to correct the gravimetrically-derived geoid in the North Sea area for its long-wavelength errors. TOPEX altimetric data (h) and gravimetric geoid heights (N) were only used in the general observation equation (2), since the SST was neglected in this study. The parametric model $\mathbf{a}_i^T \mathbf{x}$ was comprised from a simple bi-linear part with 4 parameters (1 bias, 2 tilts, 1 torsion), and a more complicated part of trigonometric polynomials with 24 coefficients. For the optimal estimation of this correction model only the external altimetric data were properly weighted, according to their precomputed standard deviations. Extensive statistical testing was also applied to validate the final adjustment results. For the refinement of land gravimetric geoid models using GPS/levelling data, Jiang and Duquenne (1996) proposed the division of the entire test area into smaller adjacent networks, in order to better model the higher frequency geoid distortions due to the insufficient local gravity data coverage and the errors in the used DTMs.

4.1.4 Vertical Datum Testing/Refinement

For such applications, the analyzed network usually contains a combination of some, or all, of the following data: (i) relative ΔH from conventional levelling, (ii) relative Δh from local GPS surveys, (iii) N or ΔN from a geoid model, (iv) absolute H and SST values at tide gauge stations, and (v) absolute h from SLR or global GPS campaigns. The above general data configuration was proposed by Kearsley et al. (1993). In their extensive study for investigating the quality of sample subsets of the Australian Height Datum (AHD), they used the following general mathematical model for known observations and unknown parameters:

$$\Delta h_{ij} = h_j - h_i + v_{\Delta h_{ij}} \quad (4.6a)$$

$$\Delta H_{ij} = H_j - H_i + v_{\Delta H_{ij}} \quad (4.6b)$$

$$\Delta N_{ij} = N_j - N_i + v_{\Delta N_{ij}} \quad (4.6c)$$

$$h_j - H_j - N_j = 0 \quad (4.6d)$$

All available observations $(\Delta h_{ij}, \Delta H_{ij}, \Delta N_{ij})$, along with their a-priori accuracy estimates, were simultaneously adjusted, using equation (4.6d) as a geometrical constraint for the unknown parameters at each station point j . For the unknown parameters, additional a-priori information can also be incorporated in the adjustment algorithm (Bayesian estimation), in the form of independent point measurements with their associated variances and possible co-variances (e.g., measurement of H at tide gauge sites). The above methodology suggests a powerful adjustment tool that can be used for vertical datum refinement/redefinition, where both geometrical (GPS, SLR) and physical (levelling, geoid, mean sea level) quantities are optimally combined in a unified fashion; see also Vaniček (1991).

Among the critical issues existing in this approach (as well as in the previously overviewed applications) is the estimation of the a-priori covariance matrices for the different data sets. Since these types of weighting measures are only used to describe the behavior of the random errors in the measurements, some augmentation of the observation equations (4.6) by additional auxiliary parametric models, describing possible systematic/datum offsets in the available data sets, should also be considered.

4.2 General Modeling Considerations

In general, equation (4.1) does not hold exactly due to not only the presence of zero-mean random errors in the height data, but also due to a number of other direct or indirect systematic effects. Since there are not usually available a-priori corrections for many of these effects, they should be individually modelled and estimated during an adjustment process. In this way, the following three general equations can be written for each point P_i in a combined GPS/Levelling/Geoid (GLG) network:

$$h_i = h_i^a + f_i^h + v_i^h, \quad H_i = H_i^a + f_i^H + v_i^H, \quad N_i = N_i^a + f_i^N + v_i^N \quad (4.7)$$

where h_i , H_i , and N_i denote the available ‘observed’ values for the GPS, orthometric and geoid heights, respectively. The superscript α denotes true values with respect to a unified geodetic datum, such that the following equation holds:

$$h_i^a - H_i^a - N_i^a = 0 \quad (4.8)$$

The f_i terms correspond to all the necessary reductions that need to be applied to the original data in order to eliminate the datum inconsistencies and other systematic errors. Finally, the v_i terms describe zero-mean random noise errors, for which a second-order stochastic model is available:

$$E\{\mathbf{v}_h \mathbf{v}_h^T\} = \mathbf{C}_h, \quad E\{\mathbf{v}_H \mathbf{v}_H^T\} = \mathbf{C}_H, \quad E\{\mathbf{v}_N \mathbf{v}_N^T\} = \mathbf{C}_N \quad (4.9)$$

For the orthometric heights, the covariance (CV) matrix \mathbf{C}_H is known from the adjustment of the levelling network. In the same way, \mathbf{C}_h can be computed from the adjustment of the GPS surveys performed at the levelled benchmarks. In the gravimetric geoid case, the covariance matrix \mathbf{C}_N is computed by simple error propagation from the original noisy data used in the geoid solution (geopotential coefficients, gravity anomalies, terrain heights); for detailed formulas, see Li and Sideris (1994). For a more realistic stochastic error model, full knowledge of the CV matrices should not be assumed. This is especially true for the geoid heights where the often vaguely known noise level of the input data (GM coefficients, gravity, DTM) and the always necessary stationary noise assumption when fast spectral techniques are employed for the computations, may cause \mathbf{C}_N to deviate considerably from reality. Hence, we will adopt the following stochastic model for the random noise effects in the three height data sets:

$$E\{\mathbf{v}_h \mathbf{v}_h^T\} = \sigma_h^2 \mathbf{Q}_h, \quad E\{\mathbf{v}_H \mathbf{v}_H^T\} = \sigma_H^2 \mathbf{Q}_H, \quad E\{\mathbf{v}_N \mathbf{v}_N^T\} = \sigma_N^2 \mathbf{Q}_N \quad (4.10)$$

where the co-factor matrices \mathbf{Q}_h , \mathbf{Q}_H , and \mathbf{Q}_N are assumed known from the sources previously indicated, and the three variance components are treated as unknown parameters controlling the validity of the a-priori random error models. One could also extend the above stochastic model a little bit more, by decomposing the covariance matrix \mathbf{C}_N into two different CV matrices with associated unknown variance components, which would correspond to the two main geoid random error sources (noisy geopotential coefficients, noisy gravity anomaly data). In this report, the set of the observation equations (4.7) and their associated stochastic model in equation (4.10) represent the basic framework upon which all the derivations in the following sections will be based.

4.3 A General Adjustment Model

Let us assume that, at each point P_i of a test network with m points, we have a triplet of height observations (h_i, H_i, N_i) , or equivalently one ‘synthetic’ observation $l_i = h_i - H_i - N_i$. By combining equations (4.7) and (4.8), we get the following observation equation for each network point:

$$l_i = h_i - H_i - N_i = (f_i^h - f_i^H - f_i^N) + (v_i^h - v_i^H - v_i^N) \quad (4.11)$$

or, in a more compact form

$$l_i = f_i + v_i^h - v_i^H - v_i^N \quad (4.12)$$

If the main objective for using such a test network is to evaluate the gravimetric geoid accuracy, then we are naturally interested in the estimation of the v_i^N terms. Since there is a stochastic model (equation 4.10) that has been associated with these terms, the values of v_i^N are supposed to reflect all the geoid random error sources that were taken into account for the computation of the matrix \mathbf{Q}_N . Furthermore, the ability to estimate the

unknown parameter σ_N^2 according to some variance component estimation algorithm (see, e.g., Rao, 1971; Rao, 1997), provides probably the most powerful statistical tool for a reliable estimate of the actual geoid noise, and a useful means of testing all the assumptions that were incorporated in the construction of the preliminary geoid error model \mathbf{Q}_N . There is still, however, an amount of geoid error which is not included in the v_i^N terms, and for which no a-priori information is available in general. We can very briefly mention: aliasing effects, improper (or omitted) terrain and density modelling, various biases in the coefficients of the geopotential model, etc. Such geoid errors, which do not follow a zero-mean random behavior, will be absorbed in the f_i correction term along with many other systematic effects in the GPS and levelling data. In the absence of any prior statistical and/or deterministic information for these error sources, filtering them out and estimating their magnitude individually is impossible.

If, on the other hand, this test network is to be used for the determination of an optimal corrector surface for future GPS/levelling applications, then the values f_i have to be estimated and spatially modeled in the best possible way. The *random noise* terms v_i^h, v_i^H, v_i^N should be left out of the modeling for such a correction surface. This can be easily realized by looking at the form of the basic observation equation in a future orthometric height network, which will utilize GPS/geoid information, as well as the computed corrector surface from our original test network, i.e.

$$h - N - c = H + v \quad (4.13)$$

where the term c represents the reduction effect of the computed correction model. A system of equations, created by taking the differences of equation (4.13) between the GPS survey points, has now to be adjusted for the optimal estimation of the orthometric height differences ΔH with respect to the local levelling datum. Correcting, prior to this adjustment, the ‘GPS/geoid observations’ for their random noise effects (which is the case if the terms v_i^h and v_i^N from equation (4.12) are included in the modeling of the corrector surface term c) makes no sense statistically. Furthermore, if the residual values

v_i^H from equation (4.12) are included in the modeling of the corrector surface, then the available original observations in equation (4.13) will be ‘corrected’ for an error source which does not even exist in them!

Let us now return to our initial observation model of equation (4.12). The correction term $f_i = f(P_i)$ represents a 2D spatial field of values, and it can be further decomposed in the general form:

$$f_i = \mathbf{a}_i^T \mathbf{x} + s_i \quad (4.14)$$

where \mathbf{a}_i is an $(n \times 1)$ vector of known coefficients, and \mathbf{x} is an $(n \times 1)$ vector of unknown deterministic parameters. The term s_i denotes some ‘residual correction’, the nature of which (deterministic or stochastic) is left unspecified for now. The final observation equation for each point in the test network will have, therefore, the form:

$$l_i = \mathbf{a}_i^T \mathbf{x} + s_i + v_i^h - v_i^H - v_i^N \quad (4.15)$$

and by using matrix notation in order to combine all the network points, we get

$$\mathbf{l} = \mathbf{A}\mathbf{x} + \mathbf{s} + \mathbf{B}\mathbf{v} \quad (4.16)$$

where

$$\mathbf{l} = [l_1 \cdots l_i \cdots l_m]^T, \quad \mathbf{s} = [s_1 \cdots s_i \cdots s_m]^T \quad (4.17a)$$

$$\mathbf{v} = [\mathbf{v}_h^T \quad \mathbf{v}_H^T \quad \mathbf{v}_N^T]^T \quad (4.17b)$$

$$\mathbf{v}_\# = [v_1^\# \cdots v_i^\# \cdots v_m^\#]^T, \quad \#: h, H, N \quad (4.17c)$$

$$\mathbf{A} = [\mathbf{a}_1 \cdots \mathbf{a}_i \cdots \mathbf{a}_m]^T \quad (4.17d)$$

$$\mathbf{B} = [\mathbf{I}_m \quad -\mathbf{I}_m \quad -\mathbf{I}_m], \quad \mathbf{I}_m: m \times m \text{ unit matrix} \quad (4.17e)$$

This final adjustment model is summarized in Box (4.1). The associated stochastic model follows from the one introduced in equation (4.10).

$$\mathbf{l} = \mathbf{Ax} + \mathbf{s} + \mathbf{Bv} \quad \mathbf{E}\{\mathbf{v}\} = \mathbf{0}$$

$$\mathbf{E}\{\mathbf{vv}^T\} = \mathbf{C}_v = \begin{bmatrix} \mathbf{C}_h & \mathbf{0} & \mathbf{0} \\ \mathbf{0} & \mathbf{C}_H & \mathbf{0} \\ \mathbf{0} & \mathbf{0} & \mathbf{C}_N \end{bmatrix} = \begin{bmatrix} \sigma_h^2 \mathbf{Q}_h & \mathbf{0} & \mathbf{0} \\ \mathbf{0} & \sigma_H^2 \mathbf{Q}_H & \mathbf{0} \\ \mathbf{0} & \mathbf{0} & \sigma_N^2 \mathbf{Q}_N \end{bmatrix}$$

$\sigma_h^2, \sigma_H^2, \sigma_N^2$: unknown variance components

Box 4.1: A General Model for GPS/Levelling/Geoid Network Adjustment

Such adjustment problems where, apart from the unknown deterministic parameters \mathbf{x} and the zero-mean random errors \mathbf{v} , there appear also some quantities \mathbf{s} that depend on an underlying unknown function (the corrector surface in our case) are very common in geodetic applications. When the emphasis is placed on the estimation of the functionals \mathbf{s} , it is traditionally called a least-squares collocation problem with unknown parameters (Moritz, 1980). In the case where the main interest is on the parameters \mathbf{x} , it is viewed as a simple least-squares adjustment problem ‘in the presence of signals’ (Dermanis, 1978 and 1984). Both approaches are of course equivalent, with an immediate relation to the classic mixed linear models of statistical theory (see, e.g., Koch, 1987).

The crucial point for the solution of the adjustment model in Box (4.1) is how to treat the signals \mathbf{s} . In a first simple deterministic approach these signals can be treated just as

additional discrete unknown parameters, and their implicit relation with the underlying unknown function is completely ignored (see, e.g., Dermanis, 1984). This approach, however, is not applicable to our specific case of eq.(4.16), because the resulting matrix of the normal equations, under the minimization principle

$$\mathbf{v}^T \mathbf{P} \mathbf{v} = \mathbf{v}_h^T \mathbf{Q}_h^{-1} \mathbf{v}_h + \mathbf{v}_H^T \mathbf{Q}_H^{-1} \mathbf{v}_H + \mathbf{v}_N^T \mathbf{Q}_N^{-1} \mathbf{v}_N = \min \quad (4.18)$$

with the weight matrix being

$$\mathbf{P} = \begin{bmatrix} \mathbf{Q}_h^{-1} & \mathbf{0} & \mathbf{0} \\ \mathbf{0} & \mathbf{Q}_H^{-1} & \mathbf{0} \\ \mathbf{0} & \mathbf{0} & \mathbf{Q}_N^{-1} \end{bmatrix}, \quad (4.19)$$

will always be singular. In order to get a unique solution, therefore, some additional constraints need to be imposed to the residual systematic corrections s_i . Two different cases will now be identified for applying these necessary constraints.

4.4 A Purely Deterministic Approach

One easy way to solve the general adjustment model in Box (4.1) is to neglect the presence of the residual correction signals \mathbf{s} . Essentially, this means that the corrector surface will be exclusively modeled by a pre-selected deterministic parametric form. In order to avoid any rank deficiency problems, the total number of the selected parameters should be always smaller than the number of the network points. In this case, the adjustment model of Box (4.1) will be reduced to the form

$$\mathbf{l} = \mathbf{A}\mathbf{x} + \mathbf{B}\mathbf{v} \quad (4.20)$$

where \mathbf{A} is some appropriate design matrix with full column rank. The final solution of equation (4.20), under the minimization principle (4.18), will be given by the equations

$$\mathbf{W} = \mathbf{I}_m - \mathbf{A} \left(\mathbf{A}^T (\mathbf{Q}_h + \mathbf{Q}_H + \mathbf{Q}_N)^{-1} \mathbf{A} \right)^{-1} \mathbf{A}^T (\mathbf{Q}_h + \mathbf{Q}_H + \mathbf{Q}_N)^{-1} \quad (4.21a)$$

$$\hat{\mathbf{x}} = \left[\mathbf{A}^T (\mathbf{Q}_h + \mathbf{Q}_H + \mathbf{Q}_N)^{-1} \mathbf{A} \right]^{-1} \mathbf{A}^T (\mathbf{Q}_h + \mathbf{Q}_H + \mathbf{Q}_N)^{-1} \mathbf{l} \quad (4.21b)$$

$$\hat{\mathbf{v}}_h = \mathbf{Q}_h (\mathbf{Q}_h + \mathbf{Q}_H + \mathbf{Q}_N)^{-1} \mathbf{W}\mathbf{l} \quad (4.21c)$$

$$\hat{\mathbf{v}}_H = - \mathbf{Q}_H (\mathbf{Q}_h + \mathbf{Q}_H + \mathbf{Q}_N)^{-1} \mathbf{W}\mathbf{l} \quad (4.21d)$$

$$\hat{\mathbf{v}}_N = - \mathbf{Q}_N (\mathbf{Q}_h + \mathbf{Q}_H + \mathbf{Q}_N)^{-1} \mathbf{W}\mathbf{l} \quad (4.21e)$$

$$\hat{\mathbf{v}}_{total} = \mathbf{B}\hat{\mathbf{v}} = \hat{\mathbf{v}}_h - \hat{\mathbf{v}}_H - \hat{\mathbf{v}}_N = \mathbf{W}\mathbf{l} \quad (4.21f)$$

In the case where we do not have available a full CV matrix for the height data noise, but only some gross estimates for their overall pointwise accuracy, a much simpler version of the above equations occurs. If we denote by q_h^2 , q_H^2 , and q_N^2 the a-priori uniform accuracy estimates for the ellipsoidal, orthometric, and geoid heights, respectively, then we get the following solution:

$$\mathbf{W} = \mathbf{I}_m - \mathbf{A} \left(\mathbf{A}^T \mathbf{A} \right)^{-1} \mathbf{A}^T \quad (4.22a)$$

$$\hat{\mathbf{x}} = \left(\mathbf{A}^T \mathbf{A} \right)^{-1} \mathbf{A}^T \mathbf{l} \quad (4.22b)$$

$$\hat{\mathbf{v}}_h = \frac{q_h^2}{q_h^2 + q_H^2 + q_N^2} \mathbf{W} \mathbf{l} \quad (4.22c)$$

$$\hat{\mathbf{v}}_H = - \frac{q_H^2}{q_h^2 + q_H^2 + q_N^2} \mathbf{W} \mathbf{l} \quad (4.22d)$$

$$\hat{\mathbf{v}}_N = - \frac{q_N^2}{q_h^2 + q_H^2 + q_N^2} \mathbf{W} \mathbf{l} \quad (4.22e)$$

From the last three equations (also from eqs.4.21c, 4.21d, 4.21e) the crucial role of the stochastic model for the random noise in the height data is obvious. It offers the means of applying an optimal filtering to the total residuals $\mathbf{B}\hat{\mathbf{v}} = \mathbf{W}\mathbf{l}$ of the adjustment by separating the noise coming from each individual height component. It is rather interesting, though a highly unrealistic case, that when stationary white noise has been assumed for all data types, the estimates for the unknown parameters $\hat{\mathbf{x}}$ and the total residuals $\mathbf{B}\hat{\mathbf{v}}$ will not depend at all on the three different noise levels q_h^2, q_H^2, q_N^2 . By applying covariance propagation to the above results, the CV matrix $\mathbf{C}_{\hat{\mathbf{x}}}$ of the adjusted

model parameters can be also determined, which should be always used to evaluate the quality of the parametric corrector surface for future GPS/levelling applications. Another useful matrix is also the cross-CV matrix between the adjusted model parameters and the adjusted residuals for the various height data sets, from which important information can be extracted regarding the correlation of the corrector surface with the available data.

The reliability of the previous results depends on (i) the suitability of the parametric model \mathbf{Ax} to describe effectively all the systematic effects in the height data sets, and (ii) the correctness of the stochastic model for the observational noise (\mathbf{Q}_h , \mathbf{Q}_H , \mathbf{Q}_N). It is, therefore, necessary to estimate also the three unknown variance components (see Box 4.1). The method of variance component estimation used in geodesy is Rao's Minimum Norm Quadratic Unbiased Estimation - MINQUE (Rao, 1971). In the geodetic literature this problem has been solved independently, for a variety of adjustment models, by many researchers; an extensive review with further references to the relevant literature is given in Grafarend (1985). The following algorithm follows the MINQUE criterion and computes optimal estimates for the unknown variance components of the ellipsoidal heights ($\hat{\sigma}_h^2$), orthometric heights ($\hat{\sigma}_H^2$), and geoid heights ($\hat{\sigma}_N^2$):

$$\hat{\sigma} = \mathbf{J}^{-1} \mathbf{k} \quad (4.23a)$$

$$\hat{\sigma} = \left[\hat{\sigma}_h^2 \quad \hat{\sigma}_H^2 \quad \hat{\sigma}_N^2 \right]^T \quad (4.23b)$$

$$k_i = \hat{\mathbf{v}}_i^T \mathbf{Q}_i^{-1} \hat{\mathbf{v}}_i \quad i, j : h, H, N \quad (4.23c)$$

$$J_{ij} = \text{tr} \left[(\mathbf{Q}_h + \mathbf{Q}_H + \mathbf{Q}_N)^{-1} \mathbf{W} \mathbf{Q}_i (\mathbf{Q}_h + \mathbf{Q}_H + \mathbf{Q}_N)^{-1} \mathbf{W} \mathbf{Q}_j \right] \quad (4.23d)$$

There are occasions, however, where the use of algorithm (4.23) may lead to negative estimates for the unknown variance components. In such cases, a modification of the MINQUE method is required (see, e.g., Sjoberg, 1984; Rao, 1997). A number of various statistical tests and subsequent iterations are finally needed in order to validate the

adjustment results. An overview of the whole adjustment procedure described in this section is given in the flowchart of Figure (4.1).

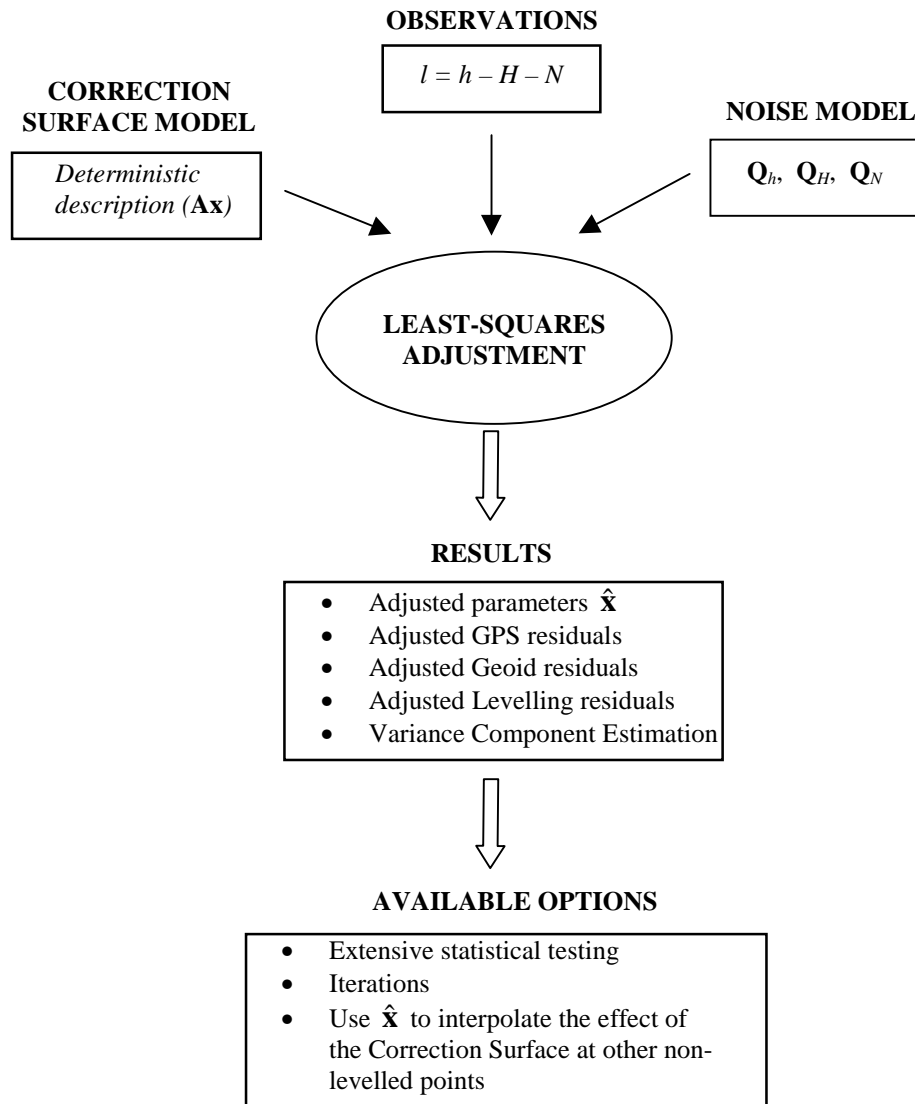


Figure 4.1: Flowchart of the Adjustment Procedure Used in the Deterministic Approach

4.5 Some Preliminary Numerical Tests of Methods Used for the Adjustment of Combined GLG Networks

A simple, preliminary numerical testing of the methods discussed thus far on the adjustment of combined GPS/levelling/geoid networks is presented in this section. The first tested method uses the traditional four-parameter transformation model approach, without any weighting applied to the data. The second method, referred here as the 'enhanced' method, was described in detail in Section 4.4 of this report.

In order to analyze these methods, real data was used to implement each method. A triplet of height information for each point in a network was required. For this, the latest (December 1998) GPS/benchmark height information in 1482 points spread across Canada was obtained from GSD. In particular, data values regarding the latitude and longitude (ϕ_i, λ_i), ellipsoidal heights with respect to NAD83 and ITRF92 geodetic datums (h_i), orthometric heights obtained from the GSD/October-1995 levelling network adjustment (H_i), and geoidal undulations from GSD95, EGM96 and OSU91A geoid models (N_i), were available at each GPS benchmark.

Given this data, two individual test networks were created, one for Western Canada ($\lambda > 110^\circ\text{W}$) and one for Eastern Canada ($\lambda < 110^\circ\text{W}$). All computations were performed using ellipsoidal heights referring to the ITRF92 geodetic datum and the geoidal undulations from the GSD95 and EGM96 geoid models

4.5.1 Western Canada

As described in the previous section, a network in Western Canada ($\lambda > 110^\circ\text{W}$), consisting of 729 points, was used to implement the two adjustment models. However, before the analysis of the results could be performed it was necessary to *clean* the data by identifying and eliminating blunders. With such a large network of points, it was determined that the best way to accomplish this task would be to plot the distribution of the observations in the network points, and visually extract any points which did not seem to fit the overall trend of this distribution. Figure (4.2) shows a histogram of the

observed residuals ($h-H-N$) in the network. The used geoid heights are coming from the GSD95 model. It is obvious from this plot that there are a few points, centered around zero, that do not fit the rest of the observations.

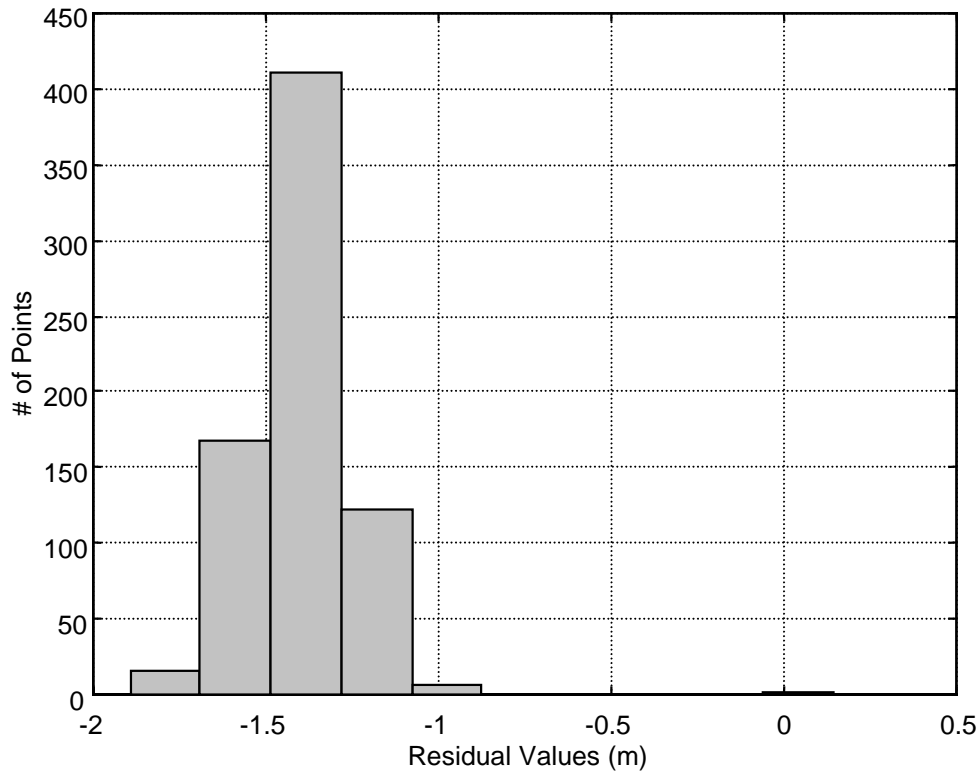


Figure 4.2: Distribution of Observed Residuals for Western Canada

Before these outliers were removed, a plot of the points versus their corresponding residual values was created using the simple four-parameter adjustment method with no data weighting and the enhanced adjustment method. The results of this are seen in Figure (4.3). The original observations are the residuals obtained by simply computing $h-H-N$ for all points in the network. From this plot, two spikes in the original observed residuals were identified as outliers. The results of the simple four-parameter adjustment method also revealed these two spikes. However, it is uncertain by looking at the simple model results, which height types are responsible for the outliers. Taking this one step further and performing the enhanced method allows us to see that the levelling residuals display the same spikes, leading to the conclusion that the outliers are due to the orthometric heights obtained from levelling. This information is valuable when cleaning

data, since it not only allows the outliers to be detected, but it also provides an indication of a possible source for the outliers.

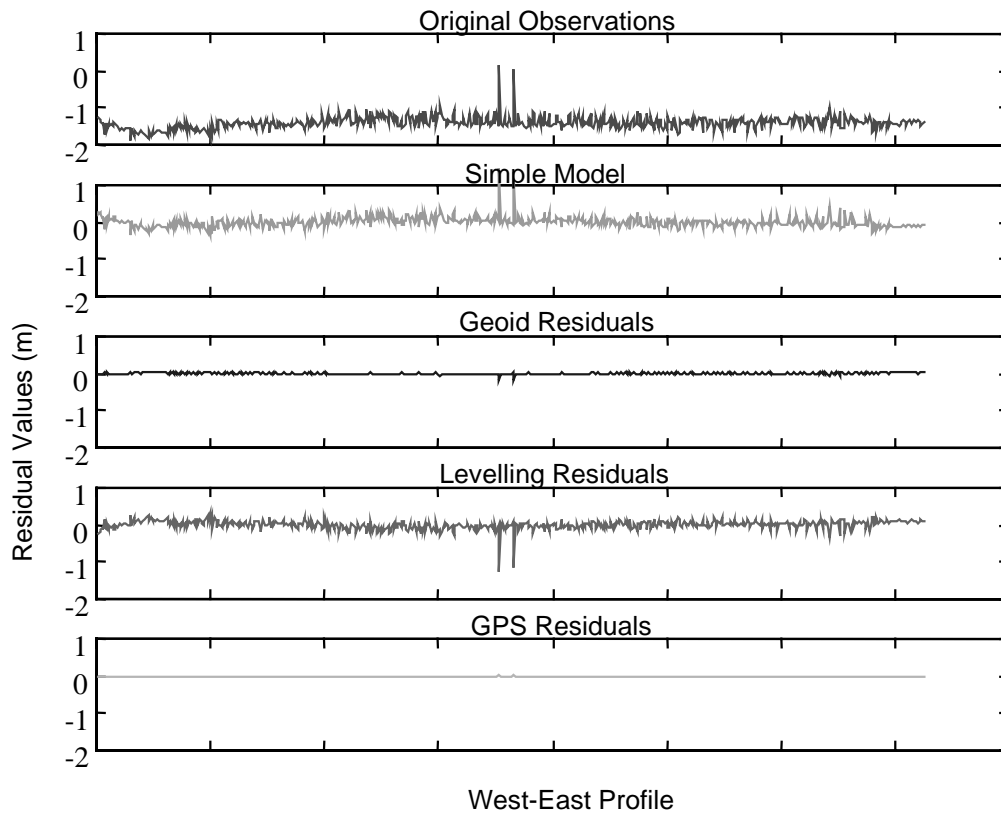


Figure 4.3: Residual Point Values for Western Canada using the Two Adjustment Methods and the GSD95 geoid model

The two blunder points were identified and eliminated from the data set. The results for the remaining 727-point network in Western Canada are provided in Figure (4.4). Two plots of the same data set, representing the west-east and north-south network profiles, are shown. This was done to visually identify possible systematic tilts in the data set. It is evident from this plot that the original observations exhibit a constant systematic effect or bias at approximately the -1.5 metre level. By applying the traditional or simple model, this systematic datum bias is removed and the zero-mean random noise effects remain. However, this plot also shows the results of the enhanced method which filters the total noise residuals obtained in the simple model and produces three individual sets of zero-mean random residuals, corresponding to the geoid model, the GPS, and the levelling heights random errors.

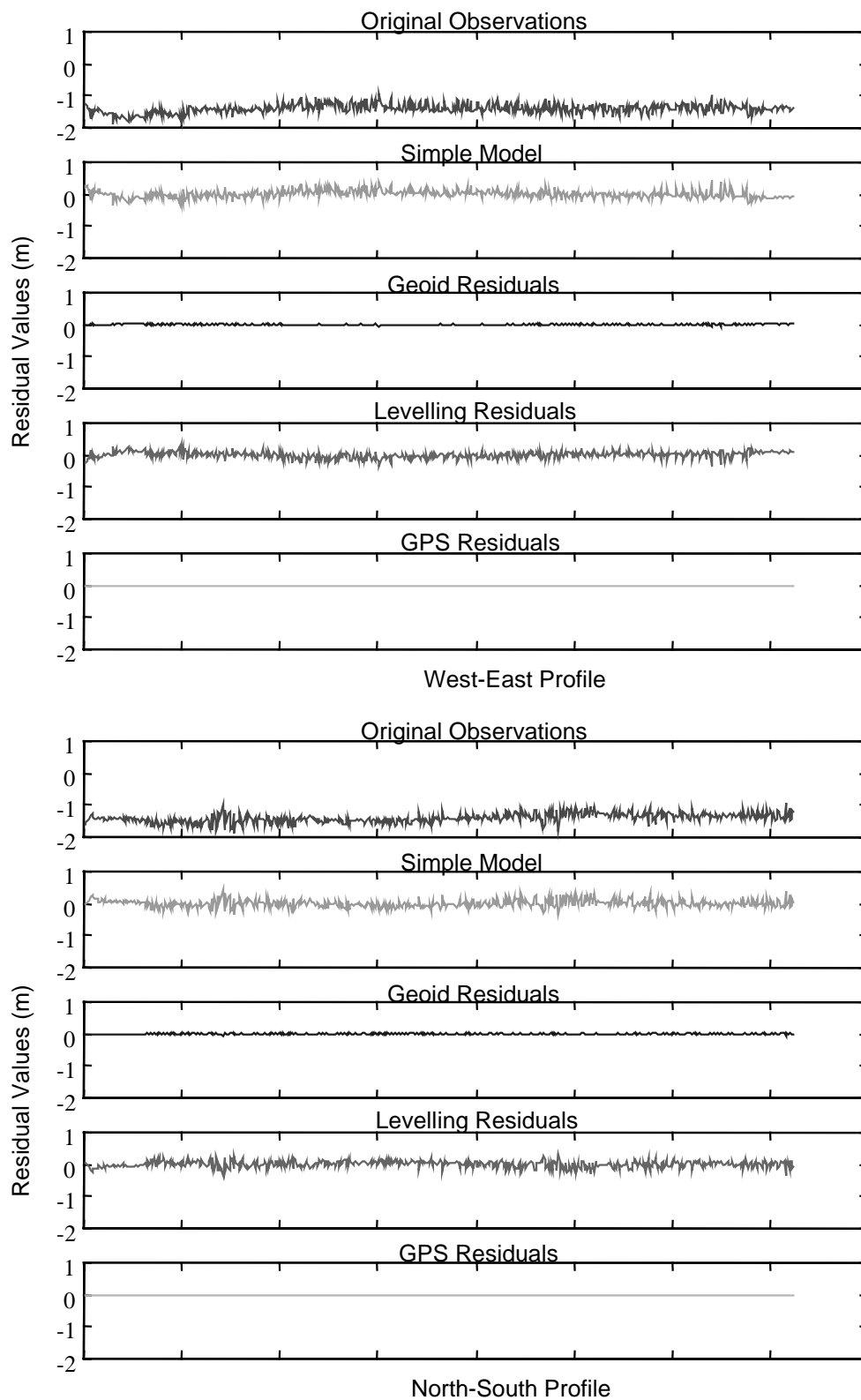


Figure 4.4: Residual Point Values for Western Canada using the Two Adjustment Methods and the GSD95 Geoid Model (outliers removed)

In order to obtain these filtered residuals (also for figure 4.3), a-priori accuracy estimates of the height data sets were used in the \mathbf{Q} matrices of the enhanced model. The GPS heights were assigned a standard deviation of 10 cm. This uniform accuracy estimate for all points was derived from the observation method and observation period (< 24 hours in most cases) which was best represented by a 10 cm accuracy level. The orthometric heights were also given a standard deviation value of 75 cm (in absolute sense). This rather large value was assigned due to the fact that some uncertainty still exists on the absolute accuracy of the vertical datum for the October 1995 national least squares adjustment. Finally, the GSD95 geoid model was used which has been shown to have an approximately 40 cm accuracy level in the mountainous areas of Western Canada.

Table (4.1) summarizes the results of the two methods for the case of Western Canada using the data and a-priori accuracy estimates described above. The main conclusions that can be drawn from Table (4.1) are that both adjustment methods are successful in removing the systematic errors introduced by the datum biases, as seen by the mean of the residuals equating to zero. The separate residuals obtained from the enhanced method show that the orthometric heights that were assigned the poorest a-priori accuracy absorb most of the random error effects. Similarly, the GPS heights that were given the lowest a-priori accuracy did not absorb much of the residual errors since they were very accurate at the outset.

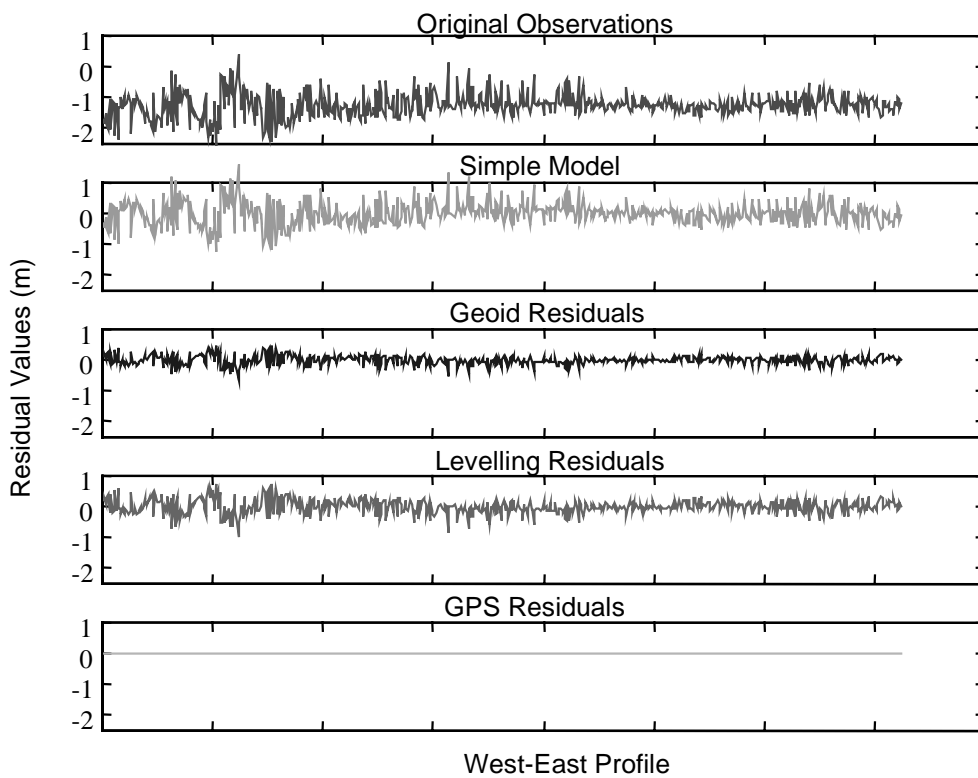
Table 4.1: Statistics for Adjusted Residuals in Western Canada

| Residual | Maximum | Minimum | Mean | σ | RMS |
|------------------------------|----------------|----------------|-------------|----------|------------|
| All values in metres | | | | | |
| Original Observations | -0.92 | -1.89 | -1.41 | 0.41 | 0.14 |
| Simple Model | 0.44 | -0.38 | 0.00 | 0.12 | 0.12 |
| GPS | 0.00 | -0.00 | 0.00 | 0.00 | 0.00 |
| Orthometric | 0.33 | -0.38 | 0.00 | 0.10 | 0.10 |
| Geoid (GSD95) | 0.05 | -0.06 | 0.00 | 0.02 | 0.02 |

To test what the sensitivity of the enhanced model is to the height data sets used, a second geoid model (EGM96) was used for the same network in Western Canada. The EGM96 geoid model is assigned an a-priori accuracy estimate of 80 cm for Western Canada

(Fotopoulos et al., 1998). The results using this second geoid model are shown in Figure (4.5), in two different profiles as was previously mentioned. Also with the use of this geoid model we see the removal of the systematic errors in the original observations by the simple and enhanced adjustment models. Once again, the levelling heights contribute the most to the residual random errors, with the geoid model being second in line.

To this point it is evident that the traditional adjustment model is successful in removing the systematic errors in Western Canada, and that the enhanced model just filters the resulting total residuals in the random errors for each height data set. However, for optimal and more reliable results, it is important that appropriate full CV matrices for the accuracy of each height data set are used for implementing the enhanced adjustment model. This will allow for a-posteriori accuracy estimates to be formed (variance component estimation) and checked against the a-priori error models. Further investigations into the quality of the accuracy estimates must be performed.



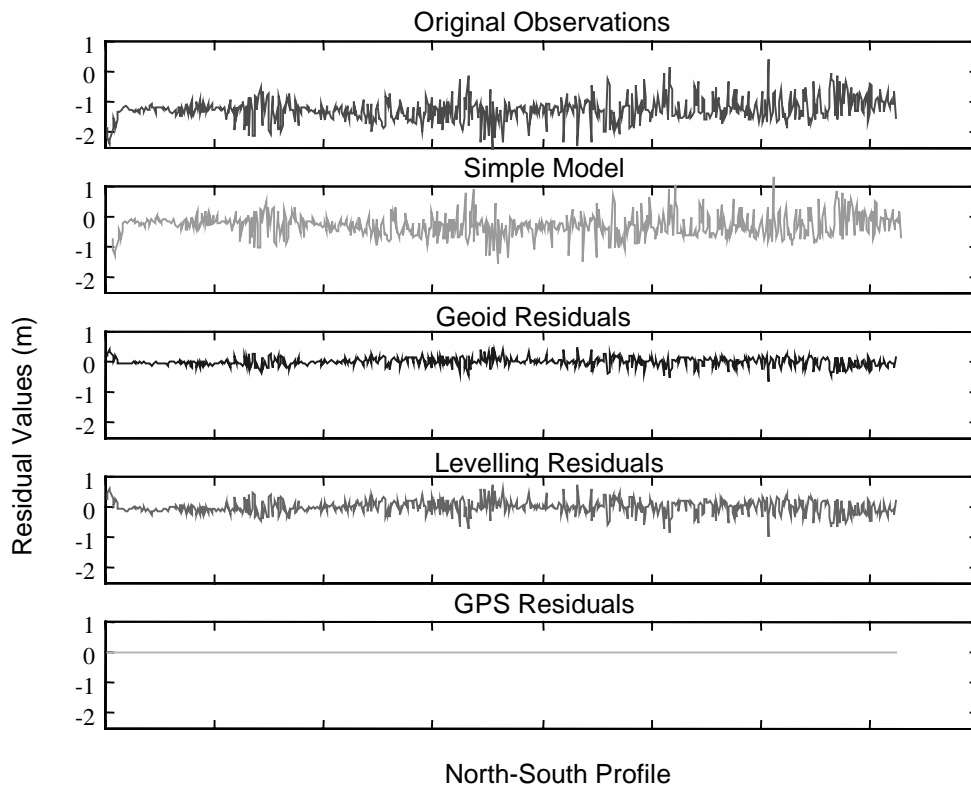


Figure 4.5: Residual Point Values for Western Canada using the Two Adjustment Methods and the EGM96 Geoid Model (outliers removed)

4.5.2 Eastern Canada

The second test network investigated using the two adjustment methods previously described was in Eastern Canada ($\lambda < 110^\circ\text{W}$) consisting of a total of 584 points. Again the distribution of the observed residuals was plotted in order to *clean* the data set of any outliers. The distribution is shown in Figure (4.6). As it is seen from this figure, although the residuals are bi-modally distributed, no outliers can be identified by visual inspection. This does not necessarily mean that outliers do not exist but more exhaustive statistical means must be used to identify the possible blunders. Since this is not the purpose of this report, it was assumed that all 584 points were valid.

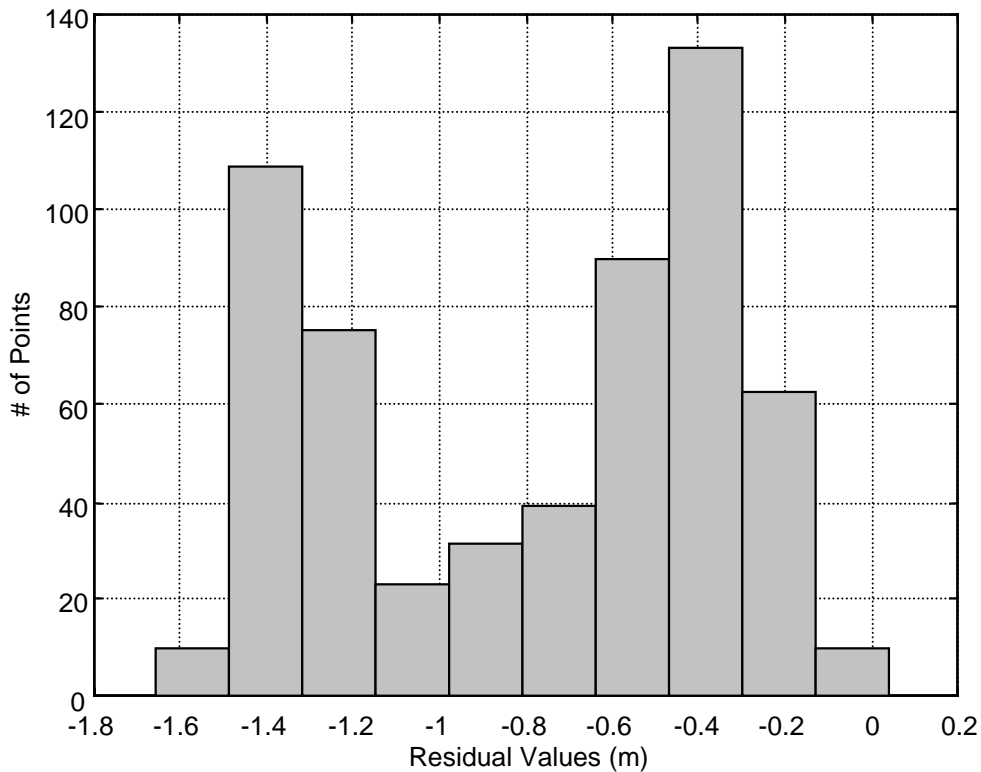


Figure 4.6: Distribution of Observed Residuals for Eastern Canada

A plot of the residual values versus the various profiles of the points in the Eastern Canadian network reveal similar results to those obtained for the Western Canadian network and are shown in Figure (4.7). Again the removal of the systematic errors by the two adjustment methods is seen. The same uniform a-priori accuracy estimates were used as those in Western Canada for all height data sets including the geoid model (GSD95). It has been shown that GSD95 performs virtually the same across Canada and thus different accuracy estimates for the Eastern network were unnecessary.

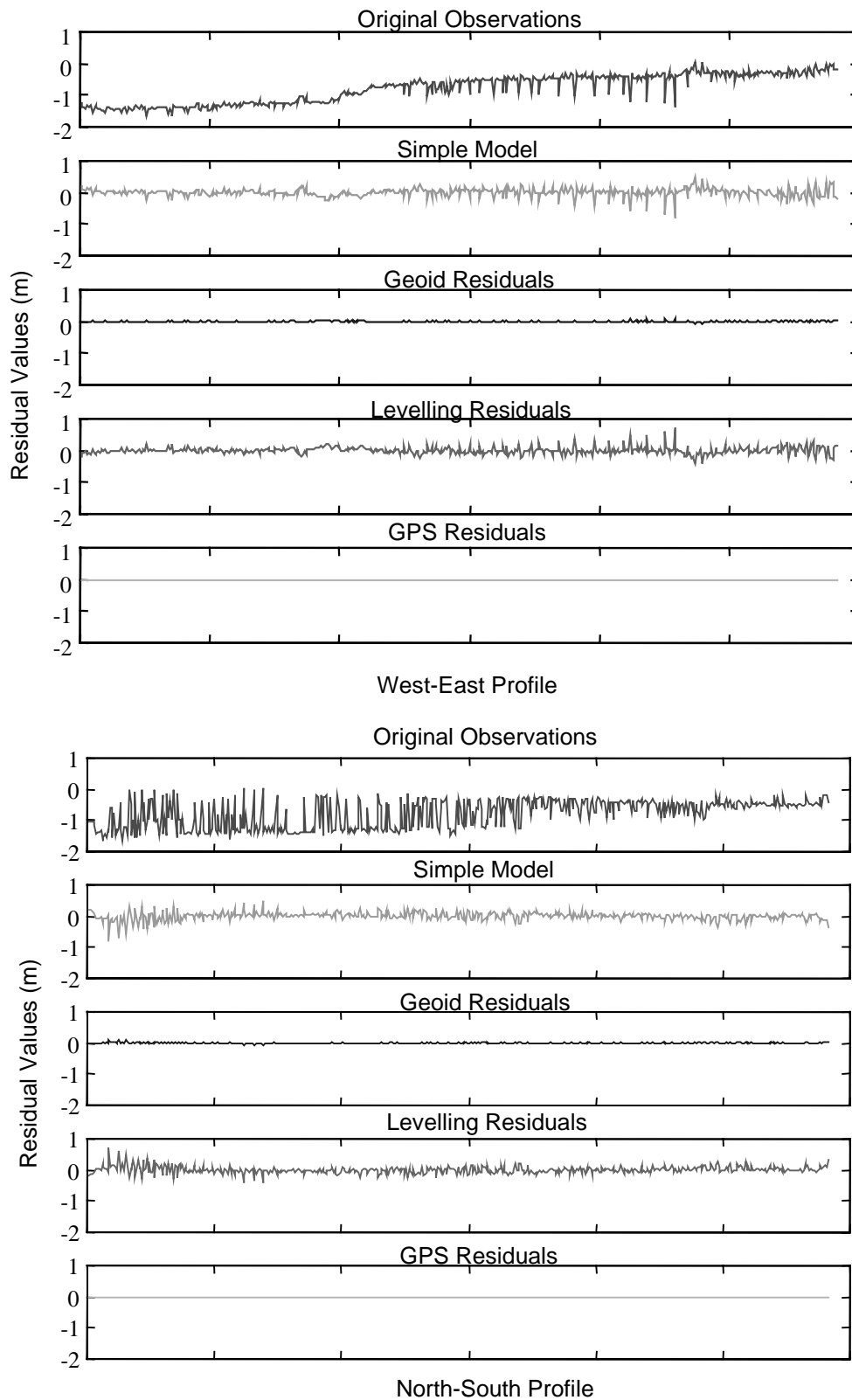


Figure 4.7: Residual Point Values for Eastern Canada using the Two Adjustment Methods (GSD95 Geoid Model)

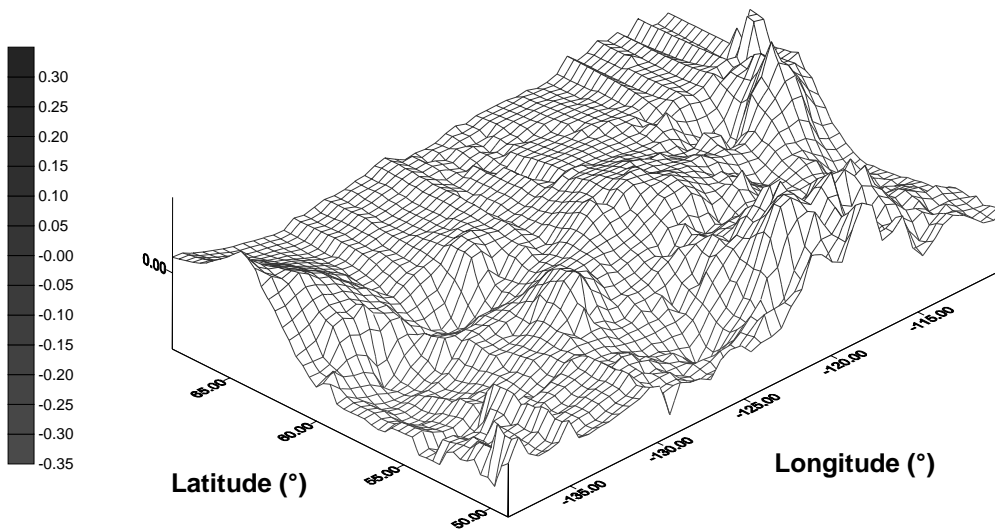
Table (4.2) summarizes the statistics computed for the residual values referring to the Eastern Canadian network. Once again, removal of the systematic errors by the adjustment models is evidenced in the mean values. The filtering of the residuals by the enhanced method is also seen in the corresponding statistical values.

Table 4.2: Statistics for Adjusted Residuals in Eastern Canada

| Residual | Maximum | Minimum | Mean | σ | RMS |
|------------------------------|----------------|----------------|-------------|----------|------------|
| All values in metres | | | | | |
| Original Observations | 0.04 | -1.67 | -0.78 | 0.44 | 0.90 |
| Simple Model | 0.49 | -0.82 | 0.00 | 0.13 | 0.13 |
| GPS | 0.00 | -0.01 | 0.00 | 0.00 | 0.00 |
| Orthometric | 0.70 | -0.42 | 0.00 | 0.11 | 0.11 |
| Geoid (GSD95) | 0.11 | -0.07 | 0.00 | 0.02 | 0.02 |

4.5.3 Surface Plots

The results presented for the enhanced model seem very promising and are a definite improvement over the traditional four-parameter model with no data weighting. In light of this more effective method of adjusting GLG networks, an additional spatial analysis was performed on the adjusted total residuals for both networks, focusing on possibly identifying a common behaviour for these values that can further be modeled by some parametric form. Surface plots of the adjusted total residuals for the Western and Eastern Canadian networks are shown in Figures (4.8) and (4.9) respectively. These plots were created in order to aid in the identification of some underlying behaviour in the adjusted total residuals that may lead to possible systematic error modelling improvements. As it is seen by the figures no dominant trend in either network exists. This reinforces our results that showed the systematic errors successfully removed for the Canadian networks by the 4-parameter transformation model. However, this analysis is vital for other areas, where the existing height data sets may not be as proficient in modelling the network region.



**Figure 4.8: Surface Plot of Adjusted Total Residuals for Western Canada
(contours in metres)**

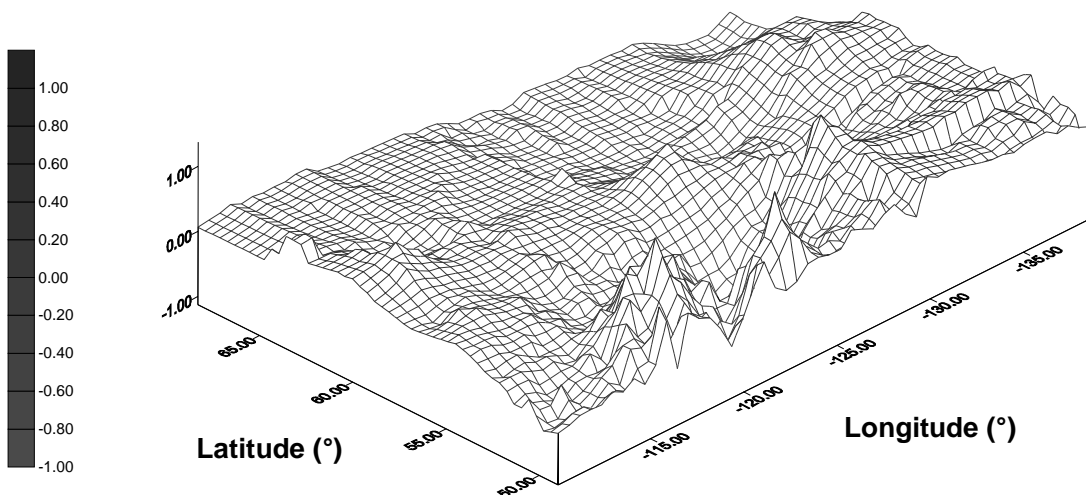


**Figure 4.9: Surface Plot of Adjusted Total Residuals for Eastern Canada
(contours in metres)**

4.6 A ‘Collocation’ Approach

The main disadvantage of the previous adjustment approach is the difficulty to find a good parametric model \mathbf{Ax} to describe *all* the possible systematic inconsistencies in the height data sets (too many effects to model). This, in turn, causes problems with respect to how reliable the results would be for the GPS/levelling/geoid noise residuals and for the corresponding variance components. The use of classical statistical testing may help to identify, to some degree, the weaknesses of a specific parametric model, but it cannot provide the means for model improvement. It should be noted that a good parametric model does not necessarily imply small values for the estimated residuals $\mathbf{B}\hat{\mathbf{v}}$, since the noise level in the original height data ($\mathbf{Q}_h, \mathbf{Q}_H, \mathbf{Q}_N$) may allow relatively large values. It is the accuracy $\mathbf{C}_{\hat{\mathbf{x}}}$ of the adjusted model parameters that should determine how good a model is, and how effectively it can be further used in future GPS/levelling applications.

Although the parameterization of the distortion effects in combined GLG networks is a very interesting topic on its own, it may be more appropriate not to try putting all the systematic errors in a pre-selected parametric form. For small networks, in particular, this should be the guiding rule, since in such cases only a small number of unknown parameters can be introduced in order to keep the degrees of freedom relatively large and the reliability of the adjustment results relatively high. Such a ‘compact’ model is of course unable to fully describe the complexity of the systematic effects and should be accompanied by additional residual corrections, which were previously introduced in the form of signals \mathbf{s} (see equation 4.16). The solution of the general adjustment model in Box (4.1) requires the incorporation of the signals \mathbf{s} in the minimization principle, which now takes the form

$$\mathbf{s}^T \mathbf{Q}_s^{-1} \mathbf{s} + \mathbf{v}_h^T \mathbf{Q}_h^{-1} \mathbf{v}_h + \mathbf{v}_H^T \mathbf{Q}_H^{-1} \mathbf{v}_H + \mathbf{v}_N^T \mathbf{Q}_N^{-1} \mathbf{v}_N = \min \quad (4.24)$$

with \mathbf{Q}_s^{-1} being an appropriate weight matrix for the unknown correction signals.

Although the solution obtained by using equation (4.24) does not necessarily have to admit a stochastic interpretation for the signal part, it is useful to consider the signals as additional stochastic parameters, just like the zero-mean random errors \mathbf{v} ; an excellent discussion on this aspect can be found in Dermanis (1984). The stochasticity of \mathbf{s} is actually necessary in the case where statistical tests related to the validity of their weighting (covariance) model \mathbf{Q}_s are to be applied.

One of the main difficulties in this approach is that the mean value $\mathbf{m}_s = E\{\mathbf{s}\}$ of the stochastic signals will not necessarily be zero, due to the systematic behavior that is supposed to exist in their values. As a result, \mathbf{m}_s should appear in the final estimation formulas if we are seeking unbiased estimators (i.e., equivalence between the least-squares principle (4.24) and the Best Linear Unbiased Estimation-BLUE for $E\{\mathbf{s}\} \neq \mathbf{0}$; for detailed formulas see, e.g., Dermanis, 1987). In order to avoid such computationally useless estimates, we can initially solve the system $\mathbf{I} = \mathbf{A}\mathbf{x} + \mathbf{s} + \mathbf{B}\mathbf{v}$ using equation (4.24) with a unit signal weight matrix. The initial solution for the signal part

$$\mathbf{W} = \mathbf{I}_m - \mathbf{A} \left(\mathbf{A}^T (\mathbf{Q}_h + \mathbf{Q}_H + \mathbf{Q}_N + \mathbf{I}_m)^{-1} \mathbf{A} \right)^{-1} \mathbf{A}^T (\mathbf{Q}_h + \mathbf{Q}_H + \mathbf{Q}_N + \mathbf{I}_m)^{-1} \quad (4.25a)$$

$$\hat{\mathbf{s}}_{init} = (\mathbf{Q}_h + \mathbf{Q}_H + \mathbf{Q}_N + \mathbf{I}_m)^{-1} \mathbf{W} \mathbf{I} \quad (4.25b)$$

can be viewed as the ‘smoothest’ residual correction field, that best fits the available observations \mathbf{I} , the selected parametric model $\mathbf{A}\mathbf{x}$, and the associated stochastic model for the random noise effects $(\mathbf{Q}_h, \mathbf{Q}_H, \mathbf{Q}_N)$.

Now, we can easily compute the overall trend in the signals \mathbf{s} by fitting some very smooth surface to the $\hat{\mathbf{s}}_{init}$ values. If we evaluate this fitted surface at the test network points, we get in general some values $\hat{\mathbf{m}}_s \neq \hat{\mathbf{s}}_{init}$. We can then create the following ‘reduced’ observations and signals:

$$\mathbf{l}_r = \mathbf{l} - \hat{\mathbf{m}}_s \quad (4.26a)$$

$$\mathbf{s}_r = \mathbf{s} - \hat{\mathbf{m}}_s \quad (4.26b)$$

It is now safe to assume that the reduced signals \mathbf{s}_r have zero mean, i.e., $E\{\mathbf{s}_r\}=\mathbf{0}$. Furthermore, the numerical values $(\hat{\mathbf{s}}_{init} - \hat{\mathbf{m}}_s)$ can be used for an empirical determination of a covariance function model describing the average spatial behavior of the reduced signals \mathbf{s}_r . In this way, we can repeat the adjustment of the model in Box (4.1), using a new ‘improved’ version for the stochastic model of the correction signals:

$$\mathbf{l}_r = \mathbf{A}\mathbf{x} + \mathbf{s}_r + \mathbf{B}\mathbf{v} \quad (4.27a)$$

$$E\{\mathbf{s}_r\} = \mathbf{0} \quad , \quad E\{\mathbf{s}_r \mathbf{s}_r^T\} = \mathbf{C}_{s_r} = \sigma_{s_r}^2 \mathbf{Q}_{s_r} \quad (4.27b)$$

The elements of the co-factor matrix \mathbf{Q}_{s_r} are computed according to the empirical CV model estimated at the previous step. An unknown variance component has been also introduced in order to diagnose any problems related to the validity of the empirical signal covariance function. The solution of the adjustment model in equation (4.27) will be given by the following unbiased estimators:

$$\mathbf{W} = \mathbf{I}_m - \mathbf{A} \left(\mathbf{A}^T (\mathbf{Q}_h + \mathbf{Q}_H + \mathbf{Q}_N + \mathbf{Q}_{s_r})^{-1} \mathbf{A} \right)^{-1} \mathbf{A}^T (\mathbf{Q}_h + \mathbf{Q}_H + \mathbf{Q}_N + \mathbf{Q}_{s_r})^{-1} \quad (4.28a)$$

$$\hat{\mathbf{x}} = \left[\mathbf{A}^T (\mathbf{Q}_h + \mathbf{Q}_H + \mathbf{Q}_N + \mathbf{Q}_{s_r})^{-1} \mathbf{A} \right]^{-1} \mathbf{A}^T (\mathbf{Q}_h + \mathbf{Q}_H + \mathbf{Q}_N + \mathbf{Q}_{s_r})^{-1} \mathbf{l}_r \quad (4.28b)$$

$$\hat{\mathbf{v}}_h = \mathbf{Q}_h (\mathbf{Q}_h + \mathbf{Q}_H + \mathbf{Q}_N + \mathbf{Q}_{s_r})^{-1} \mathbf{W} \mathbf{l}_r \quad (4.28c)$$

$$\hat{\mathbf{v}}_H = -\mathbf{Q}_H (\mathbf{Q}_h + \mathbf{Q}_H + \mathbf{Q}_N + \mathbf{Q}_{s_r})^{-1} \mathbf{W} \mathbf{l}_r \quad (4.28d)$$

$$\hat{\mathbf{v}}_N = -\mathbf{Q}_N (\mathbf{Q}_h + \mathbf{Q}_H + \mathbf{Q}_N + \mathbf{Q}_{s_r})^{-1} \mathbf{W} \mathbf{l}_r \quad (4.28e)$$

$$\hat{\mathbf{s}}_r = \mathbf{Q}_s (\mathbf{Q}_h + \mathbf{Q}_H + \mathbf{Q}_N + \mathbf{Q}_{s_r})^{-1} \mathbf{W} \mathbf{l}_r \quad (4.28f)$$

The final solution equations are similar to the ones obtained under the deterministic approach, with the only differences being (i) the use of reduced observations \mathbf{l}_r instead of the original \mathbf{l} , and (ii) the incorporation of the signal covariance matrix \mathbf{Q}_{s_r} . In the special case of stationary white noise in all three height data sets, no significant simplification of the above formulas occurs due to the appearance of the matrix \mathbf{Q}_{s_r} .

The estimation of the four unknown variance components $\hat{\sigma}_h^2, \hat{\sigma}_H^2, \hat{\sigma}_N^2, \hat{\sigma}_{s_r}^2$ follows a straightforward extension of the MINQUE algorithm (4.23) and it is omitted.

As was mentioned previously, various statistical tests and iterative solutions can be performed in order to finally validate the adjustment results. For statistical testing procedures in extended adjustment models with signals, see Dermanis and Rossikopoulos (1991) and the references given therein. In any case, a complete answer for the estimated corrector surface should include: (i) the estimated parametric model $\mathbf{A}\hat{\mathbf{x}}$, (ii) the parameters describing the non-zero mean signal trend ($\hat{\mathbf{m}}_s$ are just the values of this trend at the test network points), (iii) the estimated values for the reduced zero-mean signals $\hat{\mathbf{s}}_r$ at the network points, and (iv) a covariance model for the zero-mean signals \mathbf{s}_r . A combined use of (iii) and (iv), in a collocation-type prediction formula, is required for the prediction of the zero-mean part of the correction signal at other non-levelled points. A general flowchart for the whole computational procedure described in this section is given in Figures (4.10a) and (4.10b).

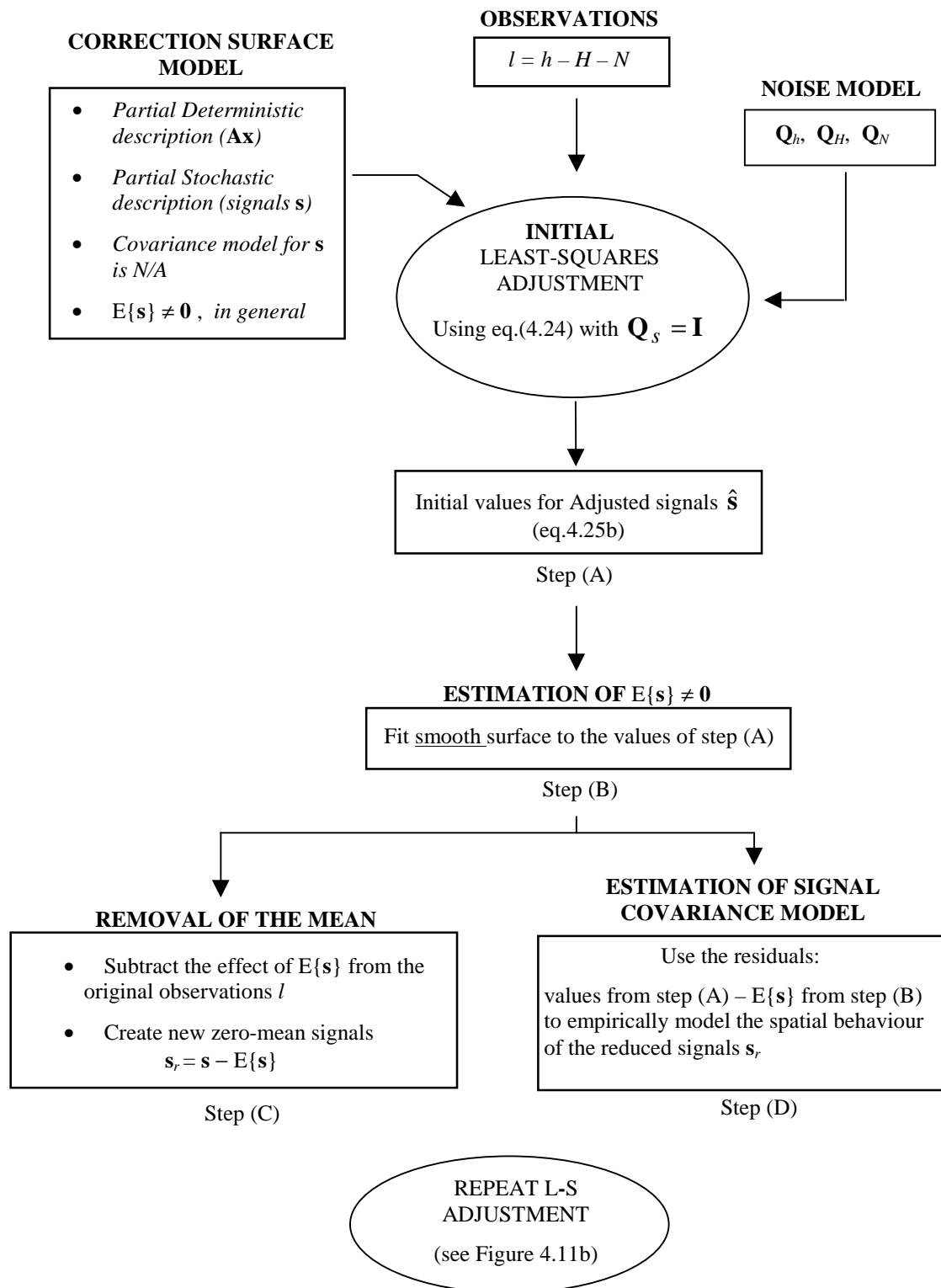


Figure 4.10a: Flowchart for the Adjustment Procedure in the ‘Collocation’ Approach

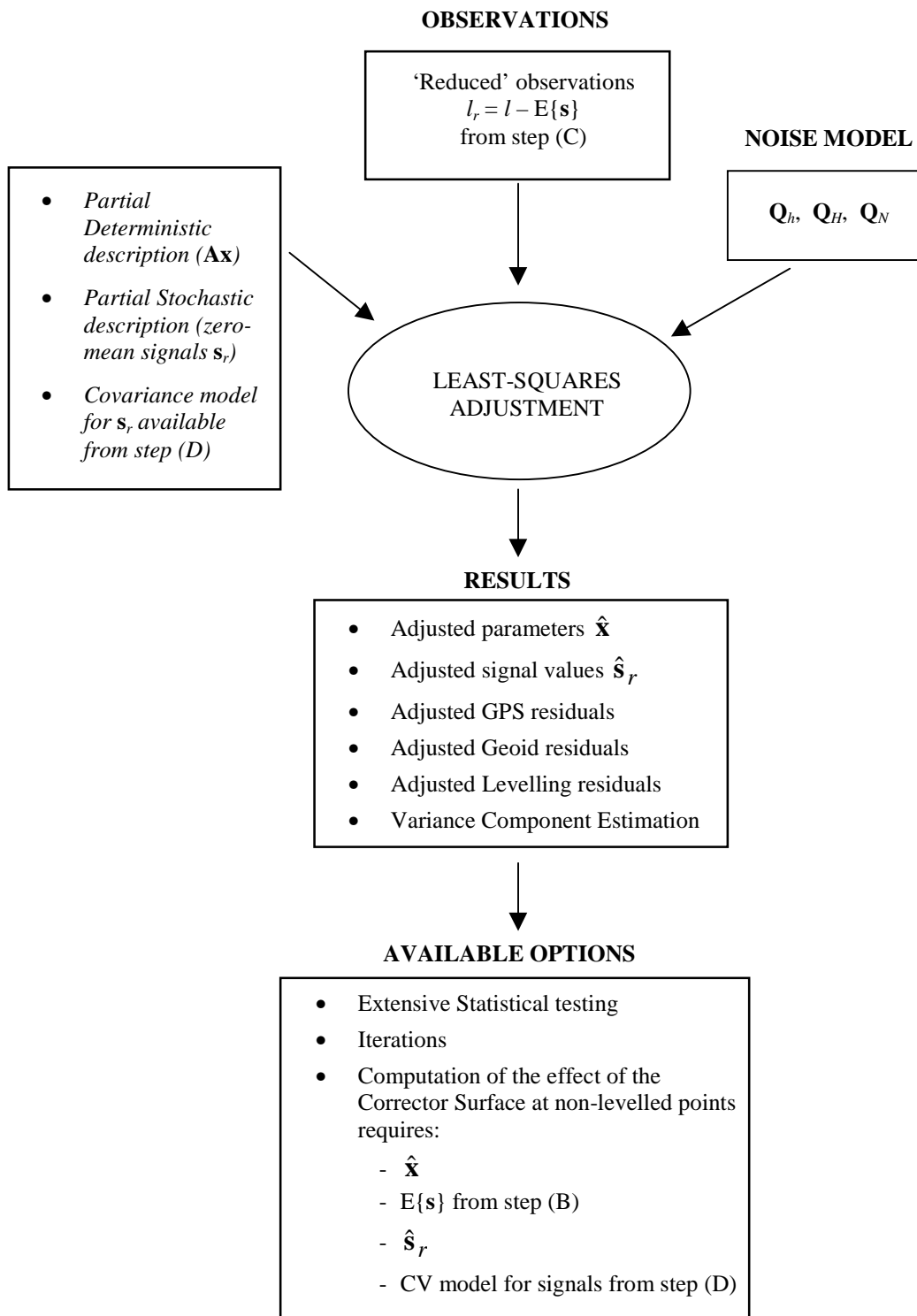


Figure 4.10b: Flowchart for the Adjustment Procedure in the ‘Collocation’ Approach (continued)

4.7 Statistical Testing in GPS/Levelling/Geoid Networks

Statistical testing for various (linear) types of hypotheses in the general adjustment models considered in this study is a very extensive and important topic. Since it is impossible to be fully covered in a single section, an attempt will only be made to draw some general lines, particularly in conjunction with the specific applications of GLG network adjustments. Relevant references in the geodetic literature that should be consulted for a more in-depth treatment of the statistical testing problem in general and extended adjustment models include Dermanis and Rossikopoulos (1991), Krakiwsky and Biacs (1990), Persson (1982), and Wei (1987). In all these references, as in the following discussion, all the stochastic components of the adjustment model (noise, signals) are assumed to be Gaussian distributed vectors of random variables.

The inherent peculiarity of GLG networks, compared to classical 1D, 2D, 3D, or integrated 1D/2D/3D geodetic networks, is a relatively high level of uncertainty regarding the validity of almost every component in the adjustment model. In most classical geodetic network problems, little doubt exists about the selected parametric models and the observational noise stochastic model, which are trusted to describe physical reality in a very consistent manner. In integrated geodetic networks, also, the necessary covariance model for the signal part can be very reliably determined by processing 'external' data (e.g., gravity anomalies, deflections of the vertical, etc.). The situation is different, however, in GLG networks where the complexity of the systematic effects involved, the often questionable gravimetric geoid error modeling, and the absence of any external information for determining a good statistical model for the residual correction signals, cause serious problems in the selection of realistic parametric, signal, and observational noise models. As a result, statistical testing in this kind of networks should not be viewed just as a 'luxury' for identifying possible outliers in the original observations, but rather as a necessity for validating and testing both the a-priori information and the modelling choices.

Before any special tests are performed for checking particular features of the general adjustment model, some global statistical test must be used first. This test will indicate if the overall model is problematic, without identifying in which specific part (parameters, signal, noise). For this type of test, the employed test statistic is

$$u = \hat{\mathbf{e}}^T \mathbf{M}^{-1} \hat{\mathbf{e}} \sim \chi_f^2 \quad (4.29)$$

where $\hat{\mathbf{e}} = \hat{\mathbf{v}}_h - \hat{\mathbf{v}}_H - \hat{\mathbf{v}}_N + \hat{\mathbf{s}}_r$, $\mathbf{M} = \mathbf{Q}_h + \mathbf{Q}_H + \mathbf{Q}_N + \mathbf{Q}_s$, and f are the degrees of freedom. In case where a fully deterministic approach has been followed for the GLG network adjustment, the terms corresponding to the signal part should be omitted from the statistic u . The acceptance of the test, for some adopted level of significance α , is verified if $\chi_f^{2(1-\alpha/2)} \leq u \leq \chi_f^{2(\alpha/2)}$.

The previous test gives an overall impression of the model validity but further testing is always required since it is possible that effects from different modelling errors cancel each other out in the computation of u . The next series of tests to be traditionally carried out are those for individual outliers in the observations, using data snooping. They are well documented in the geodetic literature, following Baarda's pioneering work. Such tests are not discussed here, their usefulness however should be always exploited after having eliminated all possible modelling errors.

Tests on the validity of the stochastic model for the observational height data noise, and on the admissibility of the empirical covariance model for the correction signals, require the estimation of the corresponding unknown variance components. A general hypothesis for variance components is (Rao and Kleffe, 1988)

$$\mathbf{H}_0 : \mathbf{H}\boldsymbol{\sigma} = \mathbf{d} \quad \text{vs.} \quad \mathbf{H}_a : \mathbf{H}\boldsymbol{\sigma} \neq \mathbf{d} \quad (4.30)$$

where $\boldsymbol{\sigma}$ is the vector containing the q unknown variance components, and \mathbf{H} is an $s \times q$ matrix of rank s . The test statistic, which follows the χ_s^2 distribution, is

$$u = \frac{1}{2} (\mathbf{H}\hat{\boldsymbol{\sigma}} - \mathbf{d})^T (\mathbf{H}\mathbf{J}^{-1}\mathbf{H}^T)^{-1} (\mathbf{H}\hat{\boldsymbol{\sigma}} - \mathbf{d}) \sim \chi_s^2 \quad (4.31)$$

and the hypothesis H_0 is accepted when $u \leq \chi_s^{2(\alpha)}$. The structure of matrix \mathbf{J} was given in (4.23d). Tests for single variance components have also appeared in the geodetic literature (see, e.g., Persson, 1982). The test

$$H_0 : \sigma_i^2 = \sigma_o^2 \quad \text{vs.} \quad H_a : \sigma_i^2 \neq \sigma_o^2 \quad (4.32)$$

is equivalent to the test

$$H_0 : u_i = \frac{k_i}{p_i \sigma_o^2} = 1 \quad \text{vs.} \quad H_a : u_i = \frac{k_i}{p_i \sigma_o^2} \neq 1 \quad (4.33)$$

where

$$k_i = \hat{\mathbf{v}}_i^T \mathbf{Q}_i^{-1} \hat{\mathbf{v}}_i \quad \text{for } i = h, H, N \quad \text{and} \quad k_i = \hat{\mathbf{s}}_r^T \mathbf{Q}_s^{-1} \hat{\mathbf{s}}_r \quad \text{for } i = s_r \quad (4.34a)$$

$$p_i = \text{tr} \left[(\mathbf{Q}_h + \mathbf{Q}_H + \mathbf{Q}_N + \mathbf{Q}_s)^{-1} \mathbf{W} \mathbf{Q}_i \right] \quad (4.34b)$$

The general structure of matrix \mathbf{W} is given in (4.28a). For GLG network adjustment without signals, all the signal-related terms in the above equations disappear. The hypothesis H_0 is accepted when

$$F_{p_i, \infty}^{1-a/2} \leq u_i \leq F_{p_i, \infty}^{a/2} \quad (4.35)$$

where F denotes centennial points of the Fisher distribution.

Another important family of statistical tests can be used to check the performance of the deterministic model for the systematic distortion effects in GLG networks. Although it would be very useful to be able to test between *different* deterministic model choices, no statistical tools are available in this direction. The only possibility is to compare ‘nested’ deterministic models, which essentially means to either test for the existence of possible additional parameters in an already adopted model (model expansion) or to test the possibility of deleting some of the already used model parameters (model shrinkage). Computationally efficient statistics have been developed for performing the above tests, which do not require the repetition of the adjustment procedure using the expanded/shrunked parametric model. All the necessary formulas can be found in Dermanis and Rossikopoulos (1991). An additional empirical tool that can be employed for a rough check of the deterministic model is the use of correlation values among the adjusted model parameters. High correlation suggests possible over-parameterization, whereas low correlation gives priority to model expansion.

A combined use of all the above mentioned tests, with parallel iterative adjustment solutions incorporating at each step in the stochastic model the previously estimated variance components and probably correcting the deterministic model, should be employed for a rigorous assessment of GLG networks. It is likely that after some iterations the variance components will be stabilized to some certain values. If, in addition, the accuracy of the adjusted model parameters is satisfactory, we can then trust the final results to contain valuable information regarding the actual gravimetric geoid noise level, and the behavior of the systematic effects that are needed to transform GPS heights to orthometric heights relative to the local vertical datum.

One final important comment should be made for the covariance model of the correction signals s_r . Apart from the straightforward empirical way of computing such a preliminary covariance model (as it was described in a previous section) and assigning a single variance component for controlling its validity, there is always the alternative to use an a-

priori linearly parameterized CV function for the zero-mean stochastic part of the distortion field:

$$C(P, Q) = \sum_k \sigma_k^2 \psi_k(P) \psi_k(Q) \quad (4.36)$$

where the ‘degree variances’ σ_k^2 play now the role of the unknown variance components, i.e.:

$$E\{\mathbf{s}_r \mathbf{s}_r^T\} = \mathbf{C}_s = \sum_k \sigma_k^2 \mathbf{Q}_k \quad (4.37a)$$

$$\mathbf{Q}_k[i, j] = \psi_k(i) \psi_k(j) \quad (4.37b)$$

The selection of a truncated basis $\{\psi_k\}$ for describing the correction field is of course an open problem. The variance component estimation and testing problem, for the signal part, is now reduced to a ‘power spectrum’ estimation and testing problem, with respect to the adopted basis. Subsequent iterations of the whole adjustment algorithm, using the newly estimated power spectrum at each step, are required in order to get a reliable answer for the various components (geoid noise, correction signals, parameters, etc.). Such an approach could eliminate the need to use additional discrete deterministic parameters \mathbf{Ax} , under the perspective of having them included in the behavior of the selected system of basis functions. The whole GLG network adjustment problem can, in this way, be reduced to a pure collocation with random noise (geodetic terminology) or random effects model (statistics theory terminology).

5. Concluding Remarks

A new geoid model (GARR98) has been computed for Canada and parts of the United States by using the EGM96 global geopotential model and local surface and marine gravity data. Terrain effects were modeled through the use of a $1 \text{ km} \times 1 \text{ km}$ DEM for all of western Canada. The overall agreement of GARR98 with the GPS/levelling data is approximately 14 cm, after datum inconsistencies have been removed via the four-parameter transformation and outliers have been eliminated from the original GPS/levelling data. This overall accuracy approximately agrees with GSD95, however differences between the two geoid models were observed when a regional analysis was applied. Also, before the four-parameter transformation was applied at the GPS benchmarks, GARR98 improved the standard deviation obtained by GSD95 by more than 100% (from 44 cm to 20cm).

The similar accuracy results between western and eastern Canada (for both GARR98 and GSD95) indicated that the strong terrain effects in the western mountainous areas were properly modelled in both geoid models. The highest level of agreement for all models is achieved in central Canada ranging from 9 cm to 6 cm for GARR98 and GSD95, respectively. For all of Canada, the two global geopotential models show similar relative accuracies up to baseline lengths of 350 km, ranging from 3.5 ppm to 0.5 ppm. In Eastern Canada, OSU91A shows slightly better relative accuracies than EGM96 for baseline lengths up to 400 km, whereas EGM96 has better overall accuracy especially in the western regions giving relative accuracies better than 1 ppm for baselines greater than 200 km.

The main differences between GARR98 and GSD95 can be attributed to the additional gravity and height data that were used in the GSD95 solution for parts of Eastern Canada (see section 2.1). This demonstrates the importance of incorporating extended gravity and height information in gravimetric geoid solutions for large areas, such as Canada, in order to achieve the level of accuracy required for substituting conventional spirit levelling by GPS techniques. In addition, advances in global geoid modelling through the inclusion of

EGM96 help towards meeting the requirements for a more accurate national geoid model. Given these improvements in terms of data and the results from our kinematic DGPS campaign, it is evident that combining GPS with an accurate geoid model may be an efficient and accurate alternative to the traditional spirit levelling techniques currently being used.

The use of combined GPS/Levelling/Geoid networks provides a very attractive evaluation scheme for the accuracy of gravimetric geoid models. At the same time, GLG networks constitute the skeleton of ‘common points’ in the attempt to find optimal transformation models between GPS and orthometric heights. These are two *different* problems which, nevertheless, can be attacked simultaneously through a unified adjustment setting. As far as the geoid evaluation problem is concerned, a GLG network adjustment can essentially be used for testing the reliability of preliminary internal geoid error models, which have been derived via error propagation from the source data and their noise used in the gravimetric solution. Variance component estimation has been proposed as a useful statistical tool for computing and testing the actual geoid noise level. The important role played by the stochastic noise model of the other two height components was also demonstrated through the derived filtering equations for the total noise residuals of the adjustment. This general approach also allows us to check individually various additive geoid error models (see comment at the end of Section 4.2). In the absence of any prior geoid error model, we can still use a unit weight matrix and get an estimate for the a-posteriori unit geoid variance.

For the problem of modeling a corrector surface for GPS-to-orthometric height transformation, it is important to filter out all the zero-mean random noise effects coming from the triplet of the height data. This is the main weakness of some of the presently available attempts for such a modelling. This correction surface will also absorb a part of the geoid long-wavelength error which does not necessarily follow a zero-mean random behavior, and it is not possible to be explicitly isolated. Two modeling alternatives have been presented for the description of the systematic correction field. These included: (a) purely discrete deterministic modelling, (b) hybrid deterministic and ‘stochastic’

modelling. Again, the tool of variance component estimation provides the statistical means to testing the admissibility of the correction field's CV model when (b) is employed.

The problem of statistical testing for various hypotheses regarding the a-priori accuracy information and the modelling choices in GLG networks needs to be addressed in more detail, especially in view of the many different levels of accuracy desired by GPS/levelling users. In this direction, the problem of optimization and design of GLG networks is another important and interesting topic that certainly needs to be explored.

The numerical analysis of two adjustment methods used in applications requiring GLG networks has revealed some interesting results regarding the nature of the height adjustment problem. The traditional four-parameter model was proven to be sufficient for removing the systematic errors introduced by the datum differences of the three height data sets for Canada. It was also shown that a more generalized or enhanced weighting scheme could be applied in order to filter the total adjusted residuals and separate the noise coming from each height component. Furthermore, the adjustment of combined GLG networks can be used for testing the a-priori error models for GPS, levelling and geoid, given full error CV matrices for all height data. Further numerical tests using the proposed methodologies as well as various geoid models must be conducted in order to reveal the true benefits achieved from adjustments of combined GLG networks.

6. Acknowledgements

The Geodetic Survey Division of Geomatics Canada provided data and financial support for this study which the authors gratefully acknowledge. Further support was provided by an NSERC grant and an Alexander von Humboldt Research Fellowship to the third author.

7. References

- De Bruigne, A.J.T., Haagmans, R.H.N., and de Min, E.J. (1997): A Preliminary North Sea Geoid Model GEONZ97, Report from Delft University of Technology, Faculty of Geodetic Engineering.
- Dermanis, A. (1978): *Adjustment of Geodetic Observations in the Presence of Signals*. International School of Advanced Geodesy, 2nd course: 'Space-Time Geodesy, Differential Geodesy, and Geodesy in the Large', Lecture Notes, Erice, Italy, May 18 - June 2, 1978.
- Dermanis, A. (1984): *Signals in Geodetic Networks*. International School of Advanced Geodesy, 3rd course: 'Design and Optimization of Geodetic Networks', Lecture Notes, Erice, Italy, April 25 - May 10, 1984.
- Dermanis, A. (1987): *Geodetic Applications of Interpolation and Prediction*. International School of Geodesy A. Marussi, 4th course: 'Applied and Basic Geodesy: Present and Future Trends', Lecture Notes, Erice, Italy, June 15-25, 1987.
- Dermanis, A. and Rossikopoulos, D. (1991): Statistical Inference in Integrated Geodesy. Paper presented at the *IUGG XXth General Assembly*, Vienna, August 11-21, 1991.
- Duquenne, H., Jiang, Z. and Lemarie, C. (1995): Geoid Determination and Levelling by GPS: Some Experiments on a Test Network. *IAG Symposia Gravity and Geoid*, No. 113, pp. 559-568.
- Featherstone, W. (1998): Do we need a Gravimetric Geoid or a Model of the Australian Height Datum to Transform GPS Heights in Australia? *The Australian Surveyor*, vol. 43, No. 4, pp. 273-280.
- Forsberg, R. and Madsen, F. (1990): High-Precision Geoid Heights for GPS Levelling. Proceedings of the 2nd *International Symposium on Precise Positioning with the Global Positioning System*, Sept. 3-7, Ottawa, Canada, 1990, pp. 1060-1074.
- Fotopoulos, G., Kotsakis, C., and Sideris, M.G. (1998): Development and Evaluation of a New Canadian Geoid Model. Paper presented at the 2nd *Joint Meeting of the IGC and the IGeC*, Trieste, Sept. 7-12, Italy, 1998.

- Grafarend, E. (1985): Variance-Covariance Estimation, Theoretical Results and Geodetic Applications. *Statistics and Decisions, Supplement Issue 2*. pp. 407-441.
- Hein, G.W. (1986): Height Determination and Monitoring with Time Using GPS Observations and Gravity Data. In: *Determination of Heights and Height Changes*, Pelzer, H. and Niemeier, W. (eds.), Contributions to the Symposium on Height Determination and Recent Vertical Crustal Movements in Western Europe, Hannover, Sept. 15-19, 1986, pp. 349-360.
- Heiskanen, W.A. and Moritz, H. (1967): *Physical Geodesy*. W.H. Freeman, San Francisco.
- Haagmans, R., de Min, E., and van Gelderen, M. (1993): Fast evaluation of convolution integrals on the sphere using 1D FFT, and a comparison with existing methods for Stokes' integral. *Manuscripta Geodaetica*, 18, pp. 227-241.
- IGeS - International Geoid Service (1997): *The Earth Gravity Model EGM96: Testing Procedures at IGeS*. Special Issue, Bulletin n.6, D.I.I.A.R., Politecnico di Milano, Italy.
- Jiang, Z. and Duquenne, H. (1996): On the combined adjustment of gravimetrically determined geoid and GPS levelling stations. *Journal of Geodesy*, No. 70, pp. 505-514.
- Kearsley, A.H.W., Ahmad, Z. and Chan, A. (1993): National Height Datums, Levelling, GPS Heights and Geoids. *Aust. J. Geod. Photogram. Surv.*, No. 59, pp. 53-88.
- Koch, K-R. (1987): *Parameter Estimation and Hypothesis Testing in Linear Models*. Springer-Verlag.
- Krakiwsky, E. and Biacs, Z.F. (1990): Least Squares Collocation and Statistical Testing. *Bull. Geod.*, 64, pp.73-87.
- Li, Y.C. and Sideris, M.G. (1994): Minimization and Estimation of Geoid Undulation Errors. *Bull. Geod.*, 68, pp. 201-219.

- Mainville, A., Forsberg, R., and Sideris, M.G. (1992): Global Positioning System Testing of Geoids Computed from Geopotential Models and Local Gravity Data: A Case Study. *Journal of Geophysical Research*, vol. 97, No. B7, pp. 11,137-11,147.
- Mainville, A., Veronneau, M., Forsberg, R. and Sideris, M.G. (1994): A Comparison of Terrain Reduction Methods in Rough Topography. Paper presented at the *Joint Meeting of the International Gravity Commission and the International Geoid Commission*, Graz, Austria, 1994.
- Mainville, A., Craymer, M., and Blackie, S. (1997): The GPS Height Transformation 1997, An Ellipsoidal-Orthometric Height Transformation for Use with GPS in Canada. *Report of Geodetic Survey Division, Geomatics Canada, Ottawa*.
- Moritz, H. (1980): *Advanced Physical Geodesy*. Herbert Wichmann Verlag, Karlsruhe.
- Pelzer, H. (1986): Height Determination – Adjustment Models for Combined Data Sets. In: *Determination of Heights and Height Changes*, Pelzer, H. and Niemeier, W. (eds.), Contributions to the Symposium on Height Determination and Recent Vertical Crustal Movements in Western Europe, Hannover, Sept. 15-19, 1986, pp. 327-340.
- Persson, C.G. (1982): Adjustment, Weight-Testing and Detection of Outliers in Mixed SFF-SFS Models. *Manuscr. Geod.*, 7, pp.299-323.
- Rao, C.R. (1971): Estimation of Variance Components - MINQUE Theory. *Journal of Multivariate Statistics*. vol. 1, pp. 257-275.
- Rao, C.R. and Kleffe, J. (1988): *Estimation of Variance Components and Applications*. North-Holland Series in Statistics and Probability, vol.3.
- Rao, P.S.R.S. (1997): *Variance Components Estimation: Mixed Models, Methodologies, and Applications*. Monographs on Statistics and Applied Probability, vol. 78, Chapman & Hall.
- Sideris, M.G. (1990): Rigorous gravimetric terrain modelling using Molodensky's operator. *Manuscr. Geod.*, 15, pp. 97-106.

- Sideris, M.G., Mainville, A., and Forsberg, R. (1992): Geoid Testing Using GPS and Levelling (or GPS Testing Using Levelling and the Geoid?). *Aust. J. Geod. Photogram. Surv.*, No.57, pp. 62-77.
- Sjoberg, L. (1984): Non-negative Variance Component Estimation in the Gauss-Helmert Adjustment Model. *Manuscr. Geod.*, 9, pp. 247-280.
- Smith, D.A. and Milbert, D.G. (1996): The GEOID96 High Resolution Geoid Height Model for the United States. *National Oceanic and Atmospheric Administration (NOAA), U.S. National Geodetic Survey, Silver Springs, MD.*
- Vaniček, P. (1991): Vertical Datum and NAVD88. *Surveying and Land Information Systems*, Vol. 51, No. 2, pp. 83-86.
- Veronneau, M. (1994): *Determination of Mean Helmert Gravity Anomalies in a Plane Approximation*. Internal Report. Geodetic Survey Division, Geomatics Canada, Dept. of Natural Resources Canada, Ottawa, Ontario.
- Veronneau, M. (1995): *An Analysis of the Gravity Measurements Used in the Determination of the 1995 Canadian Geoid Model*. Internal Report. Geodetic Survey Division, Geomatics Canada, Dept. of Natural Resources Canada, Ottawa, Ontario.
- Veronneau, M. (1996): *Canadian Geoid Model GSD95 and its Precision*. Internal Report. Geodetic Survey Division, Geomatics Canada, Dept. of Natural Resources Canada, Ottawa, Ontario.
- Wei, M. (1987): Statistical Problems in Collocation. *Manuscr. Geod.*, 12, pp. 282-289.
- Wichiencharoen, C. (1982): *The Indirect Effect on the Computation of Geoidal Undulations*. Report No.336, Dept. of Geodetic Science and Surveying, Ohio State University, Columbus, Ohio.